平成17年度 研究成果の刊行に関する一覧表

主任研究者:山下 義博

発表者氏名	論文タイトル名	発表誌名	巻号	ページ	出版年
Koinuma, K., Yamashita, Y., Liu, W., Hatanaka, H., Kurashina, K., Wada, T., Takada, S., Kaneda, R., Choi, Y.L., Fujiwara, S.I., Miyakura, Y., Nagai, H. & Mano, H.	Epigenetic silencing of AXIN2 in colorectal carcinoma with microsatellite instability	*Oncogene*	25	139-146	2006
Koinuma, K., Kaneda, R., Toyota, M., Yamashita, Y., Takada, S., Choi, Y.L., Wada, T., Okada, M., Konishi, F., Nagai, H. & Mano, H.	Screening for genomic fragments that are methylated specifically in colorectal carcinoma with a methylated MLH1 promoter	*Carcinogenesis*	26	2078-2085	2005
Kisanuki, H., Choi, Y.L., Wada, T., Moriuchi, R., Fujiwara, S.I., Kaneda, R., Koinuma, K., Ishikawa, M., Takada, S., Yamashita, Y. & Mano, H.	Retroviral expression screening of oncogenes in pancreatic ductal carcinoma	*Eur. J. Cancer*	41	2170-2175	2005
Kaneda, R., Ueno, S., Yamashita, Y., Choi, Y.L., Koinuma, K., Takada, S., Wada, T., Shimada, K. & Mano, H.	Genome-wide screening for target regions of histone deacetylases in cardiomyocytes	*Circ. Res.,*	97	210-218	2005
Ishikawa, M., Yoshida, K., Yamashita, Y., Ota, J., Takada, S., Kisanuki, H., Koinuma, K., Choi, Y.L., Kaneda, R., Iwao, T., Tamada, K., Sugano, K. & Mano, H.	Experimental trial for diagnosis of pancreatic ductal carcinoma based on gene expression profiles of pancreatic ductal cells	*Cancer Sci*	96	387-393	2005
Fujiwara, S., Yamashita, Y., Choi, Y.L., Wada, T., Kaneda, R., Takada, S., Maruyama, Y., Ozawa, K. & Mano, H.	Transforming activity of the lymphotoxin-beta receptor revealed by expression screening	*Biochem. Biophys. Res. Commun*	338	1256-1262	2005
Choi, Y.L., Moriuchi, R., Osawa, M., Iwama, A., Makishima, H., Wada, T., Kisanuki, H., Kaneda, R., Ota, J., Koinuma, K., Ishikawa, M., Takada, S., Yamashita, Y., Oshimi, K. & Mano, H	Retroviral expression screening of oncogenes in natural killer cell leukemia	*Leuk. Res*	29	943-949	2005

平成17年度 研究成果の刊行に関する一覧表

分担研究者:間野 博行

発表者氏名	論文タイトル名	発表誌名	巻号	ページ	出版年
Mano, H.	DNA micro-array analysis of myelodysplastic syndrome	*Leuk. Lymphoma*	47	9-14	2006
Koinuma, K., Yamashita, Y., Liu, W., Hatanaka, H., Kurashina, K., Wada, T., Takada, S., Kaneda, R., Choi, Y.L., Fujiwara, S.I., Miyakura, Y., Nagai, H. & Mano, H.	Epigenetic silencing of AXIN2 in colorectal carcinoma with microsatellite instability	*Oncogene*	25	139-146	2006
Takada, S., Mano, H. & Koopman, P.	Regulation of Amh during sex determination in chickens: Sox gene expression in male and female gonads	*Cell. Mol. Life Sci.*	62	2140-2146	2005
Ohki, R., Yamamoto, K., Ueno, S., Mano, H., Misawa, Y., Fuse, K., Ikeda, U. & Shimada, K.	Gene expression profiling of human atrial myocardium with atrial fibrillation by DNA microarray analysis	*Int. J. Cardiol.*	102	233-238	2005
Numata, A., Shimoda, K., Kamezaki, K., Haro, T., Kakumitsu, H., Shide, K., Kato, K., Miyamoto, T., Yamashita, Y., Oshima, Y., Nakajima, H., Iwama, A., Aoki, K., Takase, K., Gondo, H., Mano, H. & Harada, M.	Signal transducers and activators of transcription 3 augments the transcriptional activity of CCAAT/enhancer-binding protein alpha in granulocyte colony-stimulating factor signaling pathway	*J. Biol. Chem.*	280	12621-12629	2005
Koinuma, K., Kaneda, R., Toyota, M., Yamashita, Y., Takada, S., Choi, Y.L., Wada, T., Okada, M., Konishi, F., Nagai, H. & Mano, H.	Screening for genomic fragments that are methylated specifically in colorectal carcinoma with a methylated MLH1 promoter	*Carcinogenesis*	26	2078-2085	2005
Kisanuki, H., Choi, Y.L., Wada, T., Moriuchi, R., Fujiwara, S.I., Kaneda, R., Koinuma, K., Ishikawa, M., Takada, S., Yamashita, Y. & Mano, H.	Retroviral expression screening of oncogenes in pancreatic ductal carcinoma	*Eur. J. Cancer*	41	2170-2175	2005
Kaneda, R., Ueno, S., Yamashita, Y., Choi, Y.L., Koinuma, K., Takada, S., Wada, T., Shimada, K. & Mano, H.	Genome-wide screening for target regions of histone deacetylases in cardiomyocytes	*Circ. Res.*,	97	210-218	2005
Ishikawa, M., Yoshida, K., Yamashita, Y., Ota, J., Takada, S., Kisanuki, H., Koinuma, K., Choi, Y.L., Kaneda, R., Iwao, T., Tamada, K., Sugano, K. & Mano, H.	Experimental trial for diagnosis of pancreatic ductal carcinoma based on gene expression profiles of pancreatic ductal cells	*Cancer Sci*	96	387-393	2005
Fujiwara, S., Yamashita, Y., Choi, Y.L., Wada, T., Kaneda, R., Takada, S., Maruyama, Y., Ozawa, K. & Mano, H.	Transforming activity of the lymphotoxin-beta receptor revealed by expression screening	*Biochem. Biophys. Res. Commun*	338	1256-1262	2005
Choi, Y.L., Moriuchi, R., Osawa, M., Iwama, A., Makishima, H., Wada, T., Kisanuki, H., Kaneda, R., Ota, J., Koinuma, K., Ishikawa, M., Takada, S., Yamashita, Y., Oshimi, K. & Mano, H	Retroviral expression screening of oncogenes in natural killer cell leukemia	*Leuk. Res*	29	943-949	2005
間野博行.	いかにして個別化医療が可能か	*Molecular Medicine*	42	848-850	2005
間野博行.	遺伝子発現プロファイリングによる急性骨髄性白血病の予後予測	*Molecular Medicine*	42	866-871	2005
間野博行.	マイクロアレイを用いた造血器悪性腫瘍の分類と予後	総合臨床	54	1752-1755	2005
間野博行.	DNAチップ解析による造血器腫瘍診断	日本内科学会雑誌	94	2224-2230	2005
間野博行.	DNAチップによるリンパ腫解析	血液・腫瘍科	49 (Suppl. 4)	248-253	2005
間野博行.	遺伝子発現解析に基づく予後判定	医学の歩み	212	355-359	2005
間野博行.	マイクロアレイ解析による急性骨髄性白血病の予後因子の同定	Annual Review 血液		124-130	2006

平成17年度 研究成果の刊行に関する一覧表

分担研究者：菅野 健太郎

発表者氏名	論文タイトル名	発表誌名	巻号	ページ	出版年
Osawa H, Kita H, Ohnishi H, Hoshino H, Mutoh H, Ishino Y, Watanabe E, Satoh K & Sugano K	Helicobacter pylori eradication induces marked increase in H+/K+-adenosine triphosphatase expression without altering parietal cell number in human gastric mucosa	*Gut*	55	152-157	2006
Hama K, Ohnishi H, Aoki H, Kita H, Yamamoto H, Osawa H, Sato K, Tamada K, Mashima H, Yasuda H & Sugano K	Angiotensin II promotes the proliferation of activated pancreatic stellate cells by Smad7 induction through a protein kinase C pathway	*Biochem Biophys Res Commun*	340	742-750	2006
Yano T, Yamamoto H, Kita H, Sunada K, Hayashi Y, Sato H, Iwamoto M, Sekine Y, Miyata T, Kuno A, Nishimura M, Ajibe H, Ido K & Sugano K	Technical modification of the double-balloon endoscopy to access to the proximal side of the stenosis in the distal colon	*Gastrointest Endosc*	62	302-304	2005
Tamada K & Sugano K	Diagnosis and treatment of bile duct cancer--from the viewpoint of physician	*Nippon Shokakibyo Gakkai Zasshi*	102	866-872	2005
Sunada F, Yamamoto H, Kita H, Hanatsuka K, Ajibe H, Masuda M, Hirasawa T, Osawa H, Sato K, Hozumi Y & Sugano K	A case of esophageal stricture due to metastatic breast cancer diagnosed by endoscopic mucosal resection	*Jpn J Clin Oncol*	35	483-486	2005
Sugano K	Significance of the Japanese guideline for the management of gastric ulcer	*Nippon Rinsho*	63 Suppl 11	17-21	2005
Satoh K, Yamamoto H, Kawata H, Osawa H, Hanatsuka K, Kita H, Sunada K, Hirasawa T, Yoshizawa M, Ajibe H, Satoh Y, Sunada F & Sugano K	Comparison of hemostatic effects by route of H2 receptor antagonist administration following endoscopic mucosal resection in patients with neoplastic gastric lesions	*Aliment Pharmacol Ther*	21 Suppl 2	105-110	2005
Osawa H, Nakazato M, Date Y, Kita H, Ohnishi H, Ueno H, Shiiya T, Satoh K, Ishino Y & Sugano K	Impaired production of gastric ghrelin in chronic gastritis associated with Helicobacter pylori	*J Clin Endocrinol Metab*	90	10-16	2005
Osawa H, Kita H, Ohnishi H, Sugano K & Nakazato M	Plasma and gastric ghrelin levels in subjects with Helicobacter pylori infection	*Nippon Rinsho*	63 Suppl 11	127-131	2005
Osawa H, Kita H, Ohnishi H, Mutoh H, Ishino Y, Satoh K & Sugano K	Histamine-2 receptor expression in gastric mucosa before and after Helicobacter pylori cure	*Aliment Pharmacol Ther*	21 Suppl 2	92-98	2005
Mutoh H, Satoh K, Kita H, Sakamoto H, Hayakawa H, Yamamoto H, Isoda N, Tamada K, Ido K & Sugano K	Cdx2 specifies the differentiation of morphological as well as functional absorptive enterocytes of the small intestine	*Int J Dev Biol*	49	867-871	2005
Mutoh H, Sakurai S, Satoh K, Osawa H, Tomiyama T, Kita H, Yoshida T, Tamada K, Yamamoto H, Isoda N, Ido K & Sugano K	Pericryptal fibroblast sheath in intestinal metaplasia and gastric carcinoma	*Gut*	54	33-39	2005
Kita H, Yamamoto H, Nakamura T, Shirakawa K, Terano A & Sugano K	Bleeding polyp in the mid small intestine identified by capsule endoscopy and treated by double-balloon endoscopy	*Gastrointest Endosc*	61	628-629	2005
Kawamoto C, Ido K, Isoda N, Hozumi M, Nagamine N, Ono K, Sato Y, Kobayashi Y, Nagae G & Sugano K	Long-term outcomes for patients with solitary hepatocellular carcinoma treated by laparoscopic microwave coagulation	*Cancer*	103	985-993	2005
Iwamoto M, Yamamoto H, Kita H, Sunada K, Hayashi Y, Sato H & Sugano K	Double-balloon endoscopy for ileal GI stromal tumor	*Gastrointest Endosc*	62	440-441; discussion 441	2005
Ishino Y, Ido K & Sugano K	Contamination with hepatitis B virus DNA in gastrointestinal endoscope channels: risk of infection on reuse after on-site cleaning	*Endoscopy*	37	548-551	2005

Ishikawa M, Yoshida K, Yamashita Y, Ota J, Takada S, Kisanuki H, Koinuma K, Choi YL, Kaneda R, Iwao T, Tamada K, Sugano K & Mano H	Experimental trial for diagnosis of pancreatic ductal carcinoma based on gene expression profiles of pancreatic ductal cells	*Cancer Sci*	96	387-393	2005
Hayashi Y, Yamamoto H, Kita H, Sunada K, Sato H, Yano T, Iwamoto M, Sekine Y, Miyata T, Kuno A, Iwaki T, Kawamura Y, Ajibe H, Ido K & Sugano K	Non-steroidal anti-inflammatory drug-induced small bowel injuries identified by double-balloon endoscopy	*World J Gastroenterol*	11	4861-4864	2005
Haruta H, Yamamoto H, Mizuta K, Kita Y, Uno T, Egami S, Hishikawa S, Sugano K & Kawarasaki H	A case of successful enteroscopic balloon dilation for late anastomotic stricture of choledochojejunostomy after living donor liver transplantation	*Liver Transpl*	11	1608-1610	2005
Arai Y, Tamada K, Satoh Y, Wada S, Tano S, Hanatsuka K, Ohashi A & Sugano K	Ultrasonography with liquid type CalorieMate for gallbladder motility	*Nippon Shokakibyo Gakkai Zasshi*	102	1412-1416	2005
Aoki H, Ohnishi H, Hama K, Ishijima T, Satoh Y, Hanatsuka K, Ohashi A, Wada S, Miyata T, Kita H, Yamamoto H, Osawa H, Sato K, Tamada K, Yasuda H, Mashima H & Sugano K	Autocrine Loop between Transforming Growth Factor-{beta} 1and Interleukin-1{beta} through Smad3- and ERK-dependent Pathways in Rat Pancreatic Stellate Cells	*Am J Physiol Cell Physiol*			2005

[Cancer Biology & Therapy 3:1, 96-101, January 2004]; ©2004 Landes Bioscience

Research Paper

The Tyr-Kinase Inhibitor AG879, That Blocks the ETK-PAK1 Interaction, Suppresses the RAS-Induced PAK1 Activation and Malignant Transformation

Hong He[1]
Yumiko Hirokawa[1]
Aviv Gazit[2]
Yoshihiro Yamashita[3]
Hiroyuki Mano[3]
Yuko Kawakami[4]
Kawakami[4]
Ching-Yi Hsieh[5]
Hsing-Jien Kung[5]
Guillaume Lessene[6]
Jonathan Baell[6]
Alexander Levitzki[2]
Hiroshi Maruta[1,*]

[1]Ludwig Institute for Cancer Research; Royal Melbourne Hospital; Parkville/Melbourne, Australia

[2]Department of Biological Chemistry; The Alexander Silverman Institute of Life Sciences; Hebrew University of Jerusalem; Jerusalem, Israel,

[3]Division of Functional Genomics; Jichi Medical School; Tochigi, Japan

[4]La Jolla Institute for Allergy and Immunology; San Diego, California USA

[5]Cancer Center; University of California at Davis; Sacramento, California USA

[6]Walter and Eliza Hall Institute for Medical Research; Parkville/Melbourne, Australia

*Correspondence to: Hiroshi Maruta; Ludwig Institute for Cancer Research; P.O. Box 2008 Royal Melbourne Hospital; Parkville/Melbourne, Australia 3050; Tel.: 613.9341.3155; Fax: 613.9341.3104; Email: Hiroshi.maruta@ludwig.edu.au

Received 09/16/03; Accepted 10/29/03

Previously published online as a *Cancer Biology & Therapy* E-publication: http://www.landesbioscience.com/journals/cbt/abstract.php?id=643

KEY WORDS

AG879, ETK, RAS, PAK, transformation

ACKNOWLEDGEMENTS

We thank Mrs. Thao Nheu and Dr. Hong-jian Zhu for their generous gift of a doxycycline-inducible RAS transformant of NIH/3T3 cells; Dr. Yun Qiu for her generous gift of the ETK PH domain construct in a pGEX vector; Dr. Nathan Hall for his comparison of the 3D structure of the kinase domain between ETK, BTK and TEC by a molecular modelling; and Prof. Tony Burgess for his consistent support and advice throughout this work.

ABSTRACT

AG 879 has been widely used as a Tyr kinase inhibitor specific for ErbB2 and FLK-1, a VEGF receptor. The IC_{50} for both ErbB2 and FLK-1 is around 1 μM. AG 879, in combination of PP1 (an inhibitor specific for Src kinase family), suppresses almost completely the growth of RAS-induced sarcomas in nude mice. In this paper we demonstrate that AG 879 even at 10 nM blocks the specific interaction between the Tyr-kinase ETK and PAK1 (a CDC42/ Rac-dependent Ser/Thr kinase) in cell culture. This interaction is essential for both the RAS-induced PAK1 activation and transformation of NIH 3T3 fibroblasts. However, AG 879 at 10 nM does not inhibit either the purified ETK or PAK1 directly in vitro, suggesting that this drug blocks the ETK-PAK1 pathway by targeting a highly sensitive kinase upstream of ETK. Although the Tyr-kinases Src and FAK are known to activate ETK directly, Src is insensitive to AG 879, and FAK is inhibited by 100 nM AG 879, but not by 10 nM AG879. The structure-function relationship analysis of AG 879 derivatives has revealed that both thio and tert-butyl groups of AG 879, but not (thio) amide group, are essential for its biological function (blocking the ETK-PAK1 pathway), suggesting that through the (thio) amide group, AG 879 can be covalently linked to agarose beads to form a bioactive affinity ligand useful for identifying the primary target of this drug.

INTRODUCTION

PAK1, a member of CDC42/Rac-dependent Ser/Thr kinase family (PAKs), is activated by oncogenic RAS mutants such as v-Ha-RAS, and is essential for RAS-transformation of fibroblasts such as Rat-1 and NIH 3T3 cells.[1,2] Several distinct pathways appear to be essential for v-Ha-RAS-induced activation of PAK1 in these cells.[2] One of these pathways involves PI-3 kinase which produces phosphatidyl-inositol 3,4,5 trisphosphate (PIP3) that activates both CDC42 and Rac GTPases through a GDP-dissociation stimulator (GDS) called VAV. A second pathway involves PIX, an SH3 protein which binds a Pro-rich motif (residues 186-203, PAK18) located between the N-terminal GTPase-binding domain and C-terminal kinase domain of PAK1.[3] PIX binds another protein called CAT which is a substrate of Src family kinases.[4] A third pathway involves an SH2/SH3 adaptor protein called NCK.[5] The SH3 domain of NCK binds another Pro-rich motif of PAK1 located near the N-terminus, while the SH2 domain of NCK binds the Tyr-phosphorylated EGF receptor/ErbB1.[5] Thus, when ErbB1 is activated by EGF, PAK1 is translocated to the plasma membrane through NCK. The involvement of both Src family kinases and ErbB1 in the PAK1 activation is also supported by our finding that both PP1 (inhibitor of Src family kinases) and AG1478 (ErbB1-specific inhibitor) block the RAS-induced PAK1 activation and transformation in vitro and in vivo.[2,6] A fourth pathway involves ErbB2, a member of ErbB family Tyr kinases.[2] We have previously shown that AG 825 (ErbB2-specific inhibitor) blocks RAS-induced activation of PAK1 and malignant transformation with the IC_{50} around 0.35 μM.[2] A fifth pathway has been recently discovered in which RAS activates PAK1 through Tiam1, a Rac-specific GDS , in a PI-3 kinase-independent manner.[7] In this pathway, RAS directly binds Tiam1 which in turn activates Rac.[7]

Another possible pathway involves β1-integrin, FAK and ETK. β1-integrin activates the Tyr kinase FAK, which in turn phosphorylates and activates ETK,[8] a member of TEC/BTK family Tyr kinases.[9,10] ETK carries an N-terminal pleckstrin homology (PH) domain followed by a TEC homology domain.[9,10] Activated ETK binds PAK1 through the PH domain, phosphorylates and activates PAK1.[11] However, it still remains to be

clarified (1) whether RAS requires this integrin/FAK/ ETK pathway for its oncogenicity, and (2) how RAS activates this pathway.

To suppress the growth of RAS-induced sarcomas in vivo (in nude mice), we previously used AG 879, a Tyr-kinase inhibitor specific for ErbB2 and VEGF receptor FLK-1.[2,12,13] In this paper we demonstrate that AG879 inhibits selectively the activation of ETK (IC_{50} around 5 nM), blocking RAS-induced ETK-mediated activation (Tyr phosphorylation) of PAK1 to suppress RAS transformation.

MATERIALS AND METHODS

Cell Culture and Reagents. v-Ha-RAS-transformed NIH 3T3 fibroblasts (RAS cells) were grown in a standard medium, i.e., Dulbecco's modified Eagle's medium in the presence or absence of 10% fetal calf serum as described previously.[2,6] The Tyr kinase inhibitor AG879 and its derivatives (AG 306 and AG 1584) were synthesized as described previously.[12] The novel derivative GL-2002 was synthesized analogously, and full synthetic details will be published in due course. Two other AG 879 derivatives (AG 99 and AG 213) were purchased from Calbiochem (Croydon, Australia). The following antibodies were obtained from Santa Cruz Biotechnology (Santa Cruz,CA): anti-PAK1 antibody, anti-phospho-Tyr antibody (PY99) and goat-anti-ETK antibody. The rabbit anti-FAK antibody was a generous gift of Dr. David Schlaepfer (The Scripps Research Institute, La Jolla, CA). The mouse anti-ETK antibody was purchased from Becton Dickinson Biosciences (North Ryde, NSW, Australia). The rabbit anti-ETK antibody was prepared as described previously.[14]

Assay for the Effect of AG 879 on Cell Growth. The effect of AG879 on anchorage-independent growth of RAS cells was determined by seeding 10^3 cells per plate into 0.35% top agar containing different concentrations of AG879 (from 1 nM to 1 μM) and incubating for 3 weeks as described previously.[2,6,15] At the end of 3 weeks, the colonies formed in the agar were stained and counted. The effect of AG 879 on anchorage-dependent growth of RAS cells and normal NIH/3T3 fibroblasts was examined by seeding 10^3 cells per plate in the medium containing 1–100 nM AG 879, incubating for 5 days and counting as described previously.[2,6,15]

PAK and ETK Kinase Assays. For the PAK kinase assay, RAS cells were serum-starved overnight, and then treated with different concentrations of AG879 for 1 hour as described in the text. The cells were lysed in the lysis buffer (40 mM HEPES, pH 7.4, 1% Nonidet P-40, 1 mM EDTA, 100 mM NaCl, 25 mM NaF, 100 μM $NaVO_3$, 1 mM phenylmethylsulfonyl fluoride (PMSF), and 100 units/ml aprotinin). The lysates containing 1 mg of proteins (measured by Bradford assay) were immuno-precipitated with the anti-PAK1 antibody, and the immuno-precipitates were subjected to the PAK kinase assay as described previously.[1,2,6,16] The direct effect of AG 879 on PAK1 was determined in vitro, using GST-PAK1 fusion protein as described previously.[17] For ETK kinase assay, serum-starved RAS cells were lysed in a buffer containing 20 mM Tris-HCl (pH 7.5), 100 mM NaCl, 10% glycerol, 1% Nonidet P-40, 10 mM NaF, 100 μM $NaVO_3$, 1 mM PMSF, and 100 units/ml aprotinin. The cell lysates were immuno-precipitated with the rabbit anti-ETK antibody, and the ETK kinase assay was performed as described previously[8,11] using the endogenous PAK1 associated with ETK as a substrate in the presence or absence of different concentrations of AG879 or its derivatives such as AG 1584. Immuno-blotting was performed to determine the protein levels for PAK1 and ETK (see below).

Immuno-Precipitation and Immuno-Blotting. Serum-starved RAS cells were treated with different concentrations of AG879 as indicated in the text. The cells were lysed in two different lysis buffers mentioned above. The cell lysates containing 1.5–2.0 mg of protein (measured by Bradford assay) were incubated with protein A-Sepharose beads (Amersham Pharmacia Biotech) and anti-PAK1, anti-ETK or anti-FAK antibodies separately.[2,8,11,18] The proteins in immuno-precipitates were separated on 4–12% NuPage gel (Invitrogen) electrophoresis and transferred to a nitrocellulose membrane (Micron Separations, Inc.). The membranes were blocked with 10% (w/v) skim milk in phosphate-buffered saline containing 0.04% Tween20 (PBST), followed by an incubation for 1 hr at room temperature with different first antibodies as described in the text. After washing with PBST, the blots were incubated with horseradish peroxidase-conjugated anti-mouse or anti-rabbit (Bio-Rad) secondary antibodies. The bound antibodies were visualised using ECL reagents (Amersham Pharmacia Biotech). Some membranes were stripped and reblotted[19] with different antibodies as described in the text.

The ETK Baculo Viral Construct and its Affinity-Purification. The plasmid encoding the full-length ETK (residues 1-674)[14] was constructed in pBacPAK8 transfer vector (Clontech, Palo Alto, CA) and recombinant virus was made by Dr. Chi-Ying F. Huang (NHRI, Taiwan). Sf9 insect cells infected with the recombinant virus were harvested and disrupted with ice-cold lysis buffer containing 10 mM Tris pH, 7.5; 130 mM NaCl; 1% Triton X-100; 10 mM NaF; 10 mM Na phosphate; 10 mM Na pyro-phosphate and protease inhibitor cocktail (Pharmingen, San Diego, CA). From the clear supernatant of the cell lysate obtained by centrifuging at 40,000xg for 45 min, ETK was affinity-purified by the 6xHis purification kits (Cat. No. 21474K, Pharmingen, San Diego, CA) according to the supplier's instruction.

Autophosphorylation of Recombinant ETK Constructs In Vitro. GST fusion protein of human ETKC, a constitutively activated ETK mutant (residues 243–674) which lacks the N-terminal PH domain was affinity-purified from bacteria (E. coli). The GST-ETKC (0.6 μg) was incubated in the kinase buffer containing 10 μM ATP (with or without 5 μCi of [γ-^{32}P]-ATP) as described previously[8] in the presence or absence of AG879 (10 nM or 1–10 mM) at 37°C for 40 min. The auto-phosphorylation was then monitored by immuno-blotting the protein separated by the SDS-PAGE and transferred onto nitrocellulose with anti-phospho-Tyr antibody (or by radio-autography). Similarly 3 μg of full-length ETK purified from the insect cells was incubated in the buffer containing 30 mM PIPES, pH 7.0, 10 μM $MnCl^2$, 30 μM ATP, 5 μCi of [γ -^{32}P] ATP, 1 mM Na_3VO_4 for 20 min at 30°C, in the presence or absence of AG879 (10 nM–1 mM), and the auto-phosphorylation was measured by radio-autography of the proteins separated on SDS-PAGE.

Upregulation of ETK by RAS. The ETK protein levels were compared between normal NIH/3T3 cells and two distinct v-Ha-RAS transformed cell lines, excluding the possible clonal difference in the ETK levels: stable v-Ha-RAS cell line (RAS cells) and doxycycline-inducible v-Ha-RAS transformants prepared as described previously.[20,21] The lysates of both normal and RAS cells (20 μg protein of each) were subjected to SDS-PAGE and immuno-blotted by the anti-ETK antibody. In the case of doxycycline-inducible RAS transformants, cells were incubated for 2–3 days in the presence or absence of 2 μg/ml doxycycline, and each lysate (20 μg protein) was subjected to the SDS-PAGE/ immuno-blot with the anti-ETK.

RESULTS

AG879 (10 nM) Blocks the Activation of PAK1 and Suppresses RAS-Induced Malignant Transformation. AG879 was reported as an inhibitor specific for both ErbB2 and VEGF receptor FLK-1 (IC50 is around 1 mM)[12,13] and appears to be metabolically more stable than AG825 in vivo as it strongly suppresses the growth of RAS-sarcomas in nude mice.[2] However, the IC_{50} of AG879 for inhibiting PAK1 activation and RAS transformation in vitro still remained to be determined.

10 nM AG879 strongly blocks PAK1 kinase activity in RAS cells without affecting the PAK1 protein level (Fig. 1A). However, AG879 does not inhibit the kinase activity of the purified GST-PAK1 fusion protein directly even at 1 μM (Fig. 1B). These observations suggest that ErbB2 is not involved in the inactivation by AG879 of PAK1 in cells. Interestingly, AG879 also suppresses the anchorage-independent growth of RAS cells in soft agar (Fig. 1C). The IC_{50} of AG879 for the large colony formation is 1–10 nM. However, the inhibition of anchorage-independent growth by AG879 is not due to non-specific inhibition on cell growth, as at even 100

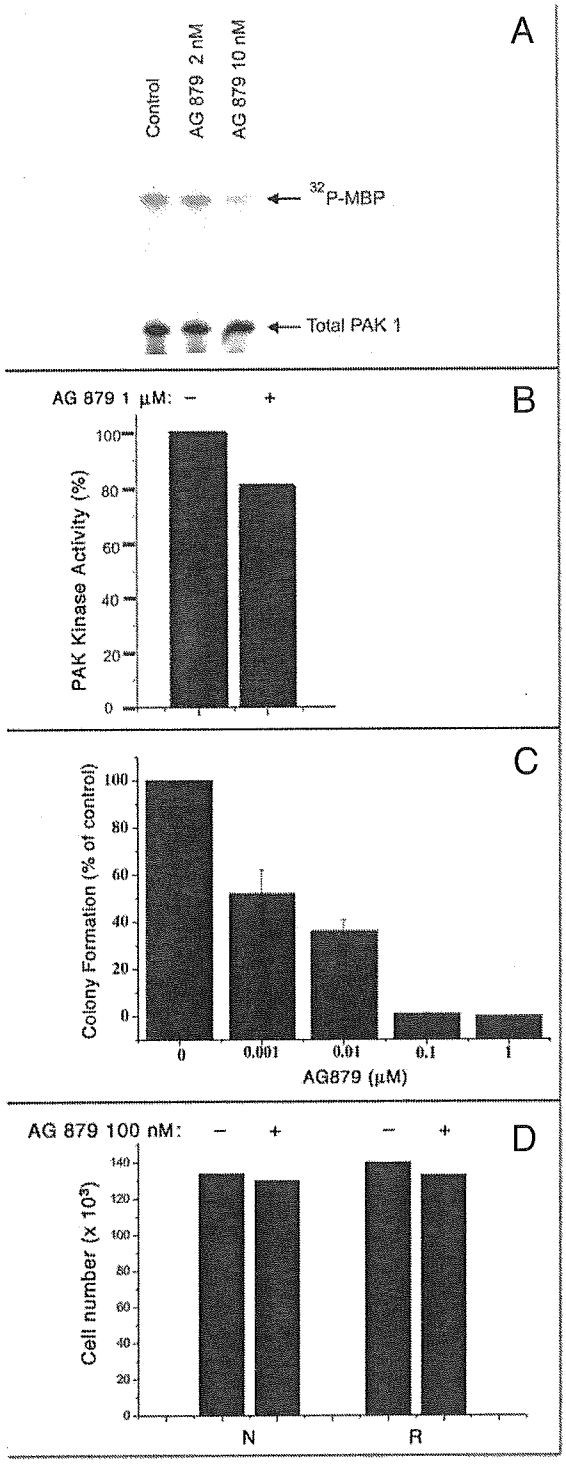

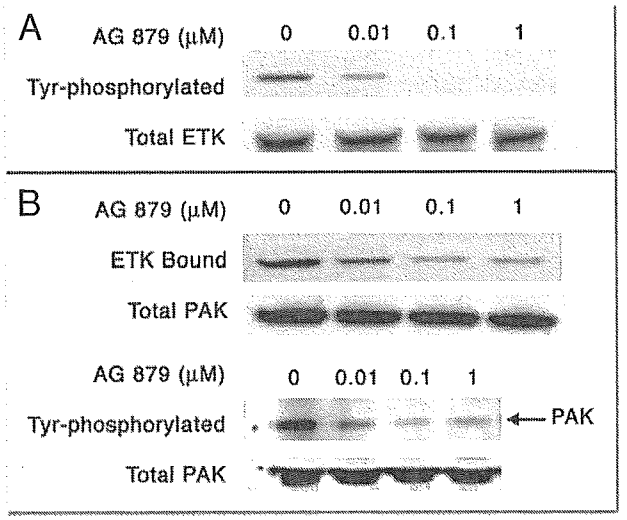

Figure 2. AG879 blocks the Tyr-phosphorylation of ETK and its association with PAK1. (A) Serum-starved RAS cells were first incubated with AG879 (0.01-1 μM) for 1hr. The cells lysates (CL) were then immuno-precipitated (IP) with the anti-ETK antibody as described under "Materials & Methods", followed by immuno-blot (IB) with anti-phospho-Tyr (PY) antibody. (B) Alternatively, the CL were IP with the anti-PAK1 (top panel) or anti-PY (bottom panel) antibodies, followed by IB with anti-ETK (top panel) or anti-PAK1 (bottom panel) antibodies. The total PAK1 protein level of the bottom panel was determined by IBing each CL directly. Similar results were obtained from two or three independent experiments.

nM AG879 does not affect the anchorage-dependent growth of either normal or RAS-transformed NIH 3T3 cells (Fig. 1D). These results suggest that the suppression by AG 879 of both RAS-induced malignant transformation and PAK1 activation is not due to blocking ErbB2, but another kinase(s) associated with PAK1.

AG879 Inhibits the Tyr-Phosphorylation of ETK and Its Association with PAK1. The Tyr-phosphorylation of PAK1 is required for its Ser/Thr kinase activity as the treatment of PAK1with a Tyr-phosphatase reduces its kinase activity.[22] Activated ETK associates with PAK1 through its PH domain and activates PAK1 by the Tyr phosphorylation.[11] To test whether the Tyr kinase activity of ETK is affected by AG879, serum-starved RAS cells were treated with AG879 (0.01–1 μM) in culture for 1hr. Cell lysates were then immuno-precipitated with the anti-ETK antibody, followed by immuno-blotting with the anti-phospho-Tyr or anti-ETK antibody. AG879 inhibits the Tyr-phosphorylation of ETK at 10 nM, but does not affect the ETK protein level (Fig. 2A). Furthermore, using the anti-PAK1 antibody, we found that AG879 significantly suppresses the ETK-PAK1 association (Fig.2B, top panel) and reduced the Tyr-phosphorylation of PAK1 in cells at 10 nM (Fig.2B, bottom panel). These results suggest that AG879 inhibits somehow the kinase activity of ETK, thus blocking its auto-phosphorylation, and association with PAK1, and the Tyr-phosphorylation of PAK1 by ETK.

AG879 Inactivates ETK In Vitro. To determine whether AG879 directly inhibits the kinase activity of ETK or not, RAS cells were lysed and

Figure 1. (A) AG879 inhibits the activation of PAK1 in cells. Serum-starved RAS cells were incubated with AG879 (0.01–10 μM) for 1hr. The cell lysates were subjected to PAK kinase assay as described under "Materials & Methods". 10 nM AG 879 clearly inhibited the PAK1 activity (phosphorylation of MBP) in cells (top panel). Similar levels of PAK1 protein were detected in all lanes as judged by immuno-blot (bottom panel). (B) PAK1 is not a direct target of AG 879. 1 μM AG 879 fails to inhibit significantly the kinase activity of GST-PAK1 in vitro. (C) AG879 inhibits anchorage-independent growth of RAS cells. RAS cells were planted in soft agar with or without AG879 (0.001–100 μM) as described under "Materials & Methods". The colony formation was measured in comparison with that of the control (non-treated) cells. Only large colonies consisting more than 100 cells per colony were counted. The presented values are the average of those obtained from two independent experiments. (D) AG 879 has no effect on the anchorage-dependent cell growth. The growth of either normal or RAS-transformed cells in liquid culture was monitored in the presence or absence of 100 nM AG 879 as described under "Materials & Methods".

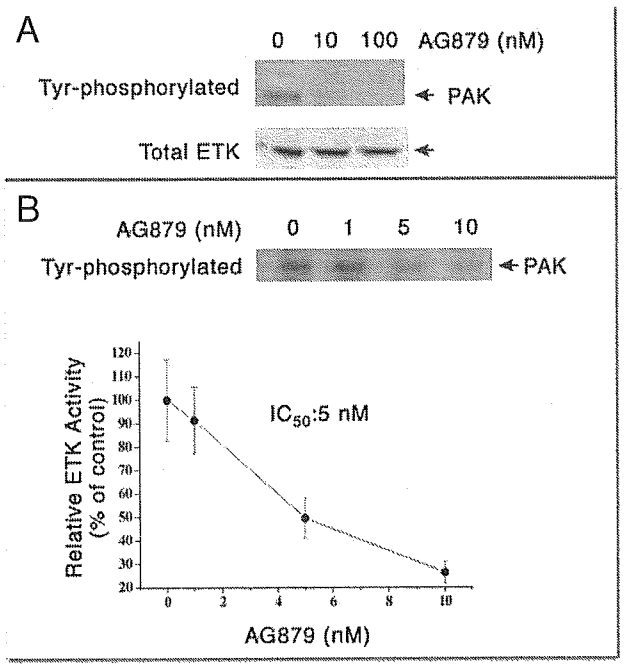

Figure 3. AG879 inhibits the kinase activity of ETK in vitro. The lysates of RAS cells were immuno-precipitated by anti-ETK antibody. The immuno-precipitates (IB) were subjected to an in vitro kinase assay in the presence or absence of AG879 (A, 10 or 100 nM; B, 1 to 10 nM) as described under "Materials & Methods". The ETK activity (Tyr-phosphorylation of PAK1) was monitored by immuno-blot (IB) with anti-PY antibody. Similar protein levels of ETK were detected in all lanes by IB with the anti-ETK antibody. Similar results were obtained from two independent experiments.

immuno-precipitated with the anti-ETK antibody. The immuno-precipitates were subjected to an in vitro kinase assay in the presence or absence of AG879 (0.001–10 μM) as described in the "Materials and Methods". AG879 (10 nM) strongly inhibits the Tyr-phosphorylation of PAK1 by

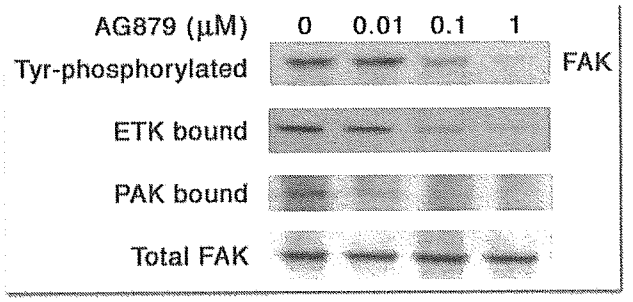

Figure 5. AG879 suppresses the Tyr-phosphorylation of FAK and its association with ETK and PAK1. Serum-starved RAS cells were incubated with AG879 (0.01–1 μM) for 1hr. The cell lysates were immuno-precipitated (IP) with anti-FAK antibody as described under "Materials & Methods", followed by immuno-blot (IB) with anti-phospho-Tyr (PY), anti-ETK or anti-PAK antibodies. Similar protein levels were detected in all lanes by IB with the anti-FAK antibody. Similar results were obtained from two independent experiments.

ETK (Fig.3A), and the IC_{50} for ETK is around 5 nM (Fig. 3B). Furthermore, AG 879 has no direct effect on any other members of TEC family kinases such as TEC, BTK or ITK, even at 10 μM in vitro (data not shown). These results suggest that ETK is so far most sensitive to the action of AG879. However, since the anti-ETK antibody could precipitates not only ETK itself, but also any proteins forming a tight complex with ETK such as PAK1 and FAK, we cannot exclude the possibility that the primary target of AG 879 might be a third Tyr-kinase which is associated with ETK, and responsible for the ETK activation.

AG879 (5 nM) Does Not Inhibit Recombinant ETK from Bacteria or Insect Cells. To clarify whether ETK itself is the primary target of ETK, two different recombinant ETK samples of human origin were purified from bacteria or insect cells: a constitutively activated mutant of ETK called ETKC (residues 243–674) which lacks the N-terminal PH domain purified from bacteria as a GST fusion protein, and full-length ETK purified from insect cells. Either the ETKC or the full-length ETK were not inhibited by AG 879 at 10 nM, although they were significantly inhibited at 1–10 μM (see Fig. 4). Furthermore, in vitro binding of PAK1 in RAS cell lysates to either the PH domain of ETK or a kinase-dead mutant of ETK (called

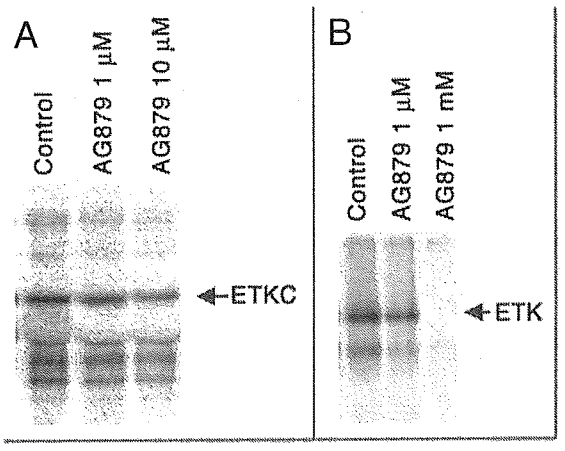

Figure 4. Recombinant ETK proteins alone are far less sensitive to AG 879 in vitro. (A) Effect of AG879 on the ETKC from bacteria. The GST-ETKC was auto-phosphorylated in the presence of AG 879 (0, 1 and 10 μM) in vitro as described under "Materials and Methods". (B) Effect of AG879 on full-length ETK from insect cells. The full-length ETK was auto-phosphorylated in the presence of AG 879 (0, 1 μM and 1mM) in vitro as described under "Materials and Methods".

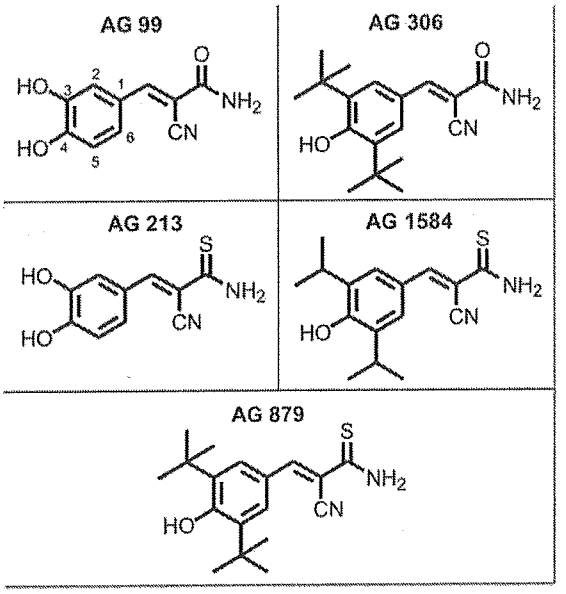

Figure 6. Chemical structure of AG 879 derivatives.

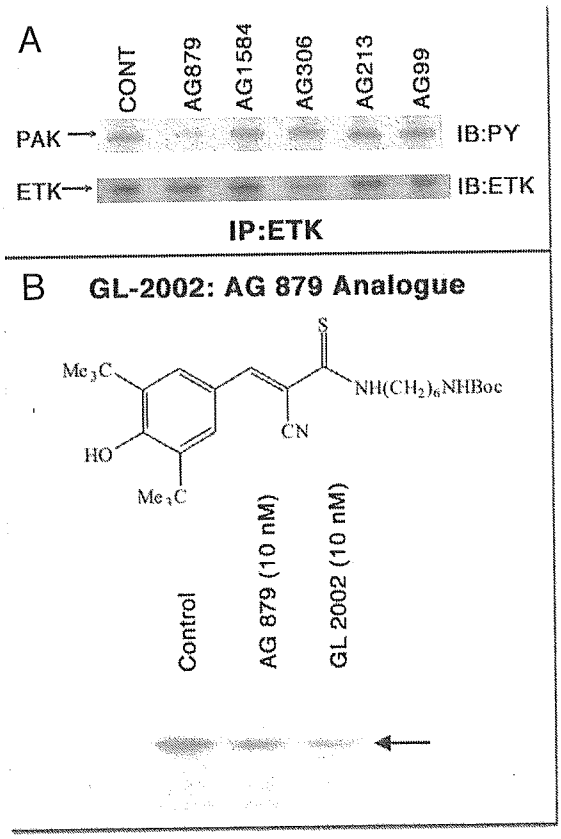

Figure 7. Anti-ETK activity of AG 879 derivatives. (A) The lysates of RAS cells were immuno-precipitated by anti-ETK antibody. The immuno-precipitates (IP) were subjected to an in vitro kinase assay in the absence of any drug (CONT) or presence of either AG879 (10 nM) or four other derivatives (10 μM) as described in Figure 3. Only AG 879 inhibits the ETK activity (Tyr-phosphorylation of PAK1) monitored by immuno-blot (IB) with anti-PY antibody. Similar protein levels of ETK were detected in all lanes by IB with the anti-ETK antibody. Similar results were obtained from two independent experiments. (B) After RAS cells were treated with either 10 nM GL-2002 or AG 879 for 1.5 hrs, each cell lysate was subjected to the in vitro PAK1 kinase assay described in Fig. 1B. GL-2002 strongly inhibited PAK1 activation as did AG 879. Similar results were obtained from three independent experiments.

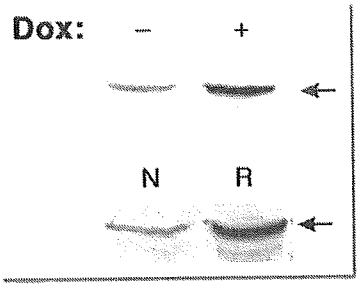

Figure 8. RAS-induced up-regulation of ETK. Upper panel: Up-regulation of ETK by the Doxycyline-induced v-Ha-RAS expression in normal NIH/3T3 cells. Dox-minus, the control (no doxycycline-added); Dox-plus, 2 μg/ml doxycycline added. Lower panel: Enhanced expression of ETK in v-Ha-RAS-transformants. N, normal NIH/3T3 cells; R, v-Ha-RAS-transformants. The arrow indicates the ETK band. Both stable and inducible RAS up-regulate the ETK protein level.

ETK/KQ) as a GST-fusion protein was not inhibited by 10 nM AG879 (Hirokawa Y, He H, Maruta H, unpublished observation, 2002). These observations altogether suggest that the primary target of AG879 is not ETK itself, but rather its associated upstream activator to be identified.

AG879 Inhibits the Tyr-Phosphorylation of FAK and Its Association with ETK and PAK1. ETK is a cytoplasmic (non-receptor) Tyr kinase which is activated at the plasma membranes.[9,10] The N-terminus of FAK shares significant sequence homology with FERM domains, which are involved in linking cytoplasmic proteins to the membranes.[23,24] It was shown recently that the activation of ETK by extracellular matrix (ECM) is regulated by FAK through the interaction between the PH domain of ETK and the FERM domain of FAK, and that activated FAK binds ETK and elevates the Tyr-phosphorylation of ETK.[8]

To test whether the FAK-ETK interaction is affected by AG879, serum-starved RAS cells were treated with AG879 (0.01–1μM). Cell lysates were then immuno-precipitated with anti-FAK antibody, followed by blotting with anti-phospho-Tyr, anti-ETK or anti-PAK1 antibodies separately. As shown in Figure 5, AG879 suppresses both the Tyr-phosphorylation of FAK and its association with ETK at 100 nM, but not at 10 nM, whereas AG879 inhibits the FAK-PAK1 interaction at 10 nM. These results suggest that PAK1 associates with FAK probably through ETK, and PAK1 can no longer interact with FAK when the PAK1-ETK complex is disrupted by AG879.

The Structure-Function Analysis of AG879 Derivatives in Inhibiting ETK. To determine which side chains of AG879 are essential for the ETK inhibition, and further screen for a more potent "ETK inhibitor", we have examined the anti-ETK activity of several AG879 derivatives shown in Figure 6. However, none of these derivatives other than AG879 itself inhibits ETK activity in vitro even at 10 μM (see Fig. 7A). These results indicate that at least both tert butyl groups at positions 3 and 5, and the thio group are absolutely essential for AG879 to inhibit ETK. Interestingly, the ErbB2-specific inhibitor AG825 is distantly related to AG879, but like AG306, lacks both the thio and tert butyl groups, and in fact shows no anti-ETK activity at even 1 μM in vitro (data not shown). However, when the free (thio) amino group of AG879 was alkylated with an amino-hexane chain, the resulting derivative called GL-2002 was still able to show a strong anti-ETK activity that blocks the PAK1 activation in RAS cells even at 10 nM (Fig. 7B), suggesting that, unlike other side chains, this free amino group of AG879 is not essential for its anti-ETK activity. Thus, we are currently generating a series of bioactive immobilized AG 879 (or its water-soluble N-hexylamine derivative, called GL-2003) by coupling them to agarose beads through the amino group so that we can use the AG879/GL-2003 bead as a ligand for fishing a high-affinity AG879-binding protein(s).

Upregulation of ETK Protein Level by RAS. How does RAS activate this integrin/FAK/ETK pathway? Although the whole picture of this mechanism still remains to be unveiled , we found that v-Ha-RAS upregulates the protein level of ETK several folds, using both doxycycline-inducible v-Ha-RAS transformants and stable v-Ha-RAS transformants derived from normal NIH/3T3 cells (see Fig. 8), clearly indicating that oncogenic RAS signalling involves ETK.

DISCUSSION

In this study, we have demonstrated that AG879 selectively inactivates the cytoplasmic Tyr kinase ETK with IC_{50} of about 5 nM. The inactivation of ETK by AG879 blocks the ETK-PAK1 interaction, thereby blocking the Tyr-phosphorylation of PAK1 and its kinase activity. Interestingly at this concentration AG879 does not inhibit directly any other kinases including FAK, PAK, ErbB2, ErbB1, TRK, TEC, BTK and ITK. However, since the IC_{50} of this drug for recombinant ETK proteins alone is 1–10 μM, instead of 5 nM, it is most likely that the primary target of AG879 is not ETK, FAK or ErbB2 themselves, but an as yet unidentified activator of ETK. Thus, we are currently identifying this highly AG879-sensitive

target among the kinases which are associated with ETK, Tyr-phosphorylate the kinase-dead (non-auto-phosphorylatable) mutant of ETK (ETK-KQ), and bind tightly to the AG879/GL-2003 beads. Our preliminary data suggest that the primary target is a Tyr-phosphorylated protein of 62 kDa (Hirokawa Y and Maruta H, unpublished observation).

ETK is required for the anchorage-independent and tumorigenic growth of human breast cancer cells.[11] Although ETK alone is not transforming, it enhances malignant transformation of NIH 3T3 cells caused by a partially activated c-Src mutant.[25] ETK can also be activated by Src family kinases and is responsible for Src activation of signal transducer and activator of transcription factor 3 (STAT3) and v-Src-induced transformation.[25] In this study we have established that ETK is essential for RAS transformation: the concentration of AG879 that inhibits both RAS-induced PAK1 activation and anchorage-independent growth is similar to the IC_{50} for ETK both in vitro and in vivo.

We have established here that RAS signalling involves ETK by demonstrating that RAS significantly up-regulates the ETK protein level. To understand further the detailed mechanism, we are currently investigating whether this regulation is at either transcriptional or translational levels or its stability (turn-over rate). In this context, it is worth noting that ETK is highly expressed in metastatic prostate and breast carcinoma cell lines such as PC3M which carry oncogenic Ki-RAS mutants.[8] Since RAS cells in general are both metastatic and angiogenic, it is conceivable that at least a part of the reason for the high expression of ETK in these cell lines might be due to the constitutive RAS activation. Thus, it would be of great interest to determine whether AG879 inhibits the metastasis of these RAS cancer cell lines in vivo.

It was suggested earlier that AG879 (also called SU0879) suppresses angiogenesis by blocking VEGF receptor FLK-1.[13] However, since the VEGF receptor also directly activates ETK[10] which is then inhibited by AG879 at 5 nM (200 times more sensitive to this drug than FLK-1), it is more likely that AG879 suppresses angiogenesis primarily by blocking ETK, rather than FLK-1. Since oncogenic RAS mutants up-regulate expression of VEGF through Raf-MEK-MAP kinase cascade,[26] and VEGF in turn activates ETK through FLK-1in endothelial cells, RAS transformation can induce angiogenesis through this paracrine pathway. Thus, it is conceivable that the suppression of RAS sarcomas growth by AG879 in mice[2] might be at least in part due to its anti-angiogenic action, (in addition to blocking the anchorage-independent growth of RAS cells per se). Interestingly it was recently shown that PAK1 is essential for angiogenesis. A cell-permeable peptide which blocks selectively the NCK-PAK1 interaction inhibits bFGF-induced angiogenesis.[27]

References

1. Tang Y, Chen Z, Ambrose D, Liu J, Gibbs JB, Chernoff J, Field J. Kinase-deficient Pak1 mutants inhibit Ras transformation of Rat-1 fibroblasts. Mol Cell Biol 1997; 17:4454-64.
2. He H, Hirokawa Y, Manser E, Lim L, Levitzki A, Maruta H. Signal therapy for RAS-induced cancers in combination of AG 879 and PP1, specific inhibitors for ErbB2 and Src family kinases, that block PAK activation. Cancer J 2001 7:191-202.
3. Manser E., Loo TH, Koh CG, et al. PAK kinases are directly coupled to the PIX family of nucleotide exchange factors. Mol Cell 1998; 1:183-92.
4. Bagrodia S, Bailey, D, Lenard, Z, et al. A tyrosine-phosphorylated protein that binds to an important regulatory region on the cool family of p21-activated kinase-binding proteins. J Biol Chem. 1999; 274:22393-400.
5. Galisteo M, Chenoff J, Su YC, et al. The adaptor protein Nck links receptor tyrosine kinases with the serine-threonine kinase Pak1. J Biol Chem 1996; 271:20997-1000.
6. He H, Hirokawa Y, Levitzki A, Maruta H. An anti-Ras cancer potential of PP1, an inhibitor specific for Src family kinases: in vitro and in vivo studies. Cancer J 2000; 6:243-8.
7. Lambert J, Lambert Q, Reuther G, Malliri A, Siderovski D, Sondek J, et al. Tiam1 mediates RAS activation of Rac by a PI-3 kinase-independent mechanism. Nat Cell Biol 2002; 4:621-5.
8. Chen R, Kim O, Li M, Xiong X, Guan JL, Kung HJ, et al. Regulation of the PH-domain-containing tyrosine kinase Etk by focal adhesion kinase through the FERM domain. Nat Cell Biol 2001; 3:439-44.
9. Qiu Y, Kung HJ. Signaling network of the Btk family kinases. Oncogene 2000; 19:5651-61.
10. Smith CI, Islam TC, Mattsson PT, Mohamed AJ, Nore BF, Vihinen M. The Tec family of cytoplasmic tyrosine kinases: mammalian Btk, Bmx, Itk, Tec, Txk and homologs in other species. Bioessays 2001; 23:436-46.
11. Bagheri-Yarmand R, Mandal M, Taludker AH, Wang RA, Vadlamudi RK, Kung HJ, Kumar R. Etk/Bmx tyrosine kinase activates Pak1 and regulates tumorigenicity of breast cancer cells. J Biol Chem 2001; 276:29403-9.
12. Levitzki A, Gazit A. Tyrosine kinase inhibition: an approach to drug development. Science 1995; 267:1782-8.
13. Strawn L, McMahon G, App H, Schreck R, et al. Flk-1 as a target for tumor growth inhibition. Cancer Res 1996; 56:3540-5.
14. Qiu Y, Robinson D, Pretlow T, Kung HJ. Etk/Bmx, a tyrosine kinase with a pleckstrin-homology domain, is an effector of phosphatidylinositol 3'-kinase and is involved in interleukin 6-induced neuroendocrine differentiation of prostate cancer cells. Proc Natl Acad Sci USA 1998; 95:3644-9.
15. Maruta H, Holden J, Sizeland A, D'Abaco G. The residues of Ras and Rap proteins that determine their GAP specificities. J Biol Chem 1991; 266:11661-8.
16. Obermeier A, Ahmed S, Manser E, Yen SC, Hall C, Lim L. PAK promotes morphological changes by acting upstream of Rac. EMBO J 1998; 17:4328-39.
17. Nheu T, He H, Hirokawa Y, Tamaki K, et al. The K252a derivatives, inhibitors for the PAK/MLK kinase family, selectively block the growth of RAS transformants. Cancer J 2002; 8:328-35.
18. Bellis SL, Miller JT, Turner CE. Characterization of tyrosine phosphorylation of paxillin in vitro by focal adhesion kinase. J Biol Chem 1995; 270:17437-41.
19. He H, Levitzki A, Zhu HJ, Walker F, Burgess A, Maruta H. Platelet-derived growth factor requires epidermal growth factor receptor to activate p21-activated kinase family kinases. J Biol Chem 2001; 276: 26741-4.
20. Zhu HJ, Iaria J, Sizeland A. Smad7 differentially regulates TGF-β-mediated signalling pathways. J Biol Chem 1999; 274:32258-64.
21. Zhu HJ, Nheu T, Cheng HC, Iaria J, Simpson R, Maruta H, Burgess AW. Oncogenic RAS transformation downregulates the expression of the PTEN tumor suppressor. Cancer Res 2003; In press.
22. McManus MJ, Boerner JL, Danielsen AJ, Wang Z, Matsumura F, Maihle NJ. An oncogenic epidermal growth factor receptor signals via a p21-activated kinase-caldesmon-myosin phosphotyrosine complex. J Biol Chem 2000; 275:35328-34.
23. Chishti AH, Kim AC, Marfatia SM, et al. The FERM domain: a unique module involved in the linkage of cytoplasmic proteins to the membrane. Trends Biochem Sci 1998; 23:281-2.
24. Girault JA, Labesse G, Mornon JP, Callebaut I. The N-termini of FAK and JAKs contain divergent band 4.1 domains. Trends Biochem Sci 1999; 24:54-7.
25. Tsai YT, Su YH, Fang SS, Huang TN, Qiu Y, Jou YS, Shih HM, Kung HJ, Chen RH. Etk, a Btk family tyrosine kinase, mediates cellular transformation by linking Src to STAT3 activation. Mol Cell Biol 2000; 20:2043-54.
26. Grugel S, Finkenzeller G, Weindel K, et al. Both v-Ha-Ras and v-Raf stimulate expression of the vascular endothelial growth factor in NIH 3T3 cells. J Biol Chem. 1995;270:25915-9.
27. Kiosses W, Hood J, Yang S, et al. A dominant-negative PAK peptide inhibits angiogenesis. Circ Res 2002; 90:697-702.

Leukemia (2004) 18, 556–565

www.nature.com/leu

DNA microarray analysis of natural killer cell-type lymphoproliferative disease of granular lymphocytes with purified CD3$^-$CD56$^+$ fractions

YL Choi[1,2], H Makishima[3], J Ohashi[4], Y Yamashita[1], R Ohki[1], K Koinuma[1], J Ota[1,5], Y Isobe[2], F Ishida[3], K Oshimi[2] and H Mano[1,5]

[1]*Division of Functional Genomics, Jichi Medical School, Kawachigun, Tochigi, Japan;* [2]*Division of Hematology, Department of Medicine, Juntendo University School of Medicine, Tokyo, Japan;* [3]*Second Department of Internal Medicine, Shinshu University School of Medicine, Matsumoto, Nagano, Japan; and* [4]*Department of Human Genetics, Graduate School of Medicine, University of Tokyo, Tokyo, Japan;* [5]*CREST, JST, Saitama, Japan*

Natural killer (NK) cell-type lymphoproliferative disease of granular lymphocytes (LDGL) is characterized by the outgrowth of CD3$^-$CD16/56$^+$ NK cells, and can be further subdivided into two distinct categories: aggressive NK cell leukemia (ANKL) and chronic NK lymphocytosis (CNKL). To gain insights into the pathophysiology of NK cell-type LDGL, we here purified CD3$^-$CD56$^+$ fractions from healthy individuals ($n=9$) and those with CNKL ($n=9$) or ANKL ($n=1$), and compared the expression profiles of >12 000 genes. A total of 15 'LDGL-associated genes' were identified, and a correspondence analysis on such genes could clearly indicate that LDGL samples share a 'molecular signature' distinct from that of normal NK cells. With a newly invented class prediction algorithm, 'weighted distance method', all 19 samples received a clinically matched diagnosis, and, furthermore, a detailed cross-validation trial for the prediction of normal or CNKL status could achieve a high accuracy (77.8%). By applying another statistical approach, we could extract other sets of genes, expression of which was specific to either normal or LDGL NK cells. Together with sophisticated statistical methods, gene expression profiling of a background-matched NK cell fraction thus provides us a wealth of information for the LDGL condition.
Leukemia (2004) **18,** 556–565. doi:10.1038/sj.leu.2403261
Published online 22 January 2004
Keywords: LDGL; DNA microarray; correspondence analysis

Introduction

Lymphoid cells (10–15%) in peripheral blood (PB) are characterized by the presence of multiple azurophilic granules in pale blue cytoplasm, referred to as large granular lymphocytes (LGLs). Such LGLs originate either from CD3$^+$ T cells or CD3$^-$CD16/56$^+$ natural killer (NK) cells,[1] and sustained outgrowth of LGLs has been designated as lymphoproliferative disease of granular lymphocytes (LDGL),[2] granular lymphocyte-proliferative disorders (GLPD)[3] or LGL leukemia (LGLL).[4]

NK cell-type LDGL can be further subdivided into two distinct categories, that is, aggressive NK cell leukemia (ANKL) and chronic NK lymphocytosis (CNKL).[5] The former is a clonal disorder of NK cells with a very poor outcome. Mono- or oligoclonal Epstein–Barr virus (EBV) genome can be frequently found in an episomal position in these NK cells,[6] suggesting a pathogenetic role of EBV in this disorder. The leukemic NK cells are often refractory to chemotherapeutic reagents, and multiple organ failure is common to ANKL patients.

In contrast, a chronic, indolent course is characteristic to CNKL. Individuals with CNKL are often symptom-free with infrequent fever, arthralgias, and cytopenia, and their NK cells are rarely positive for EBV genome.[7,8] Although the clonality of CNKL cells is still obscure partly due to the limited availability of assessment procedures, one study with X chromosome-linked gene analysis failed to detect clonality in the affected NK cells,[9] suggesting a reactive, rather than a neoplastic, nature of CNKL condition. This hypothesis is further supported by the fact that splenectomy can lead to a sustained elevation of PB NK cell count *in vivo*.[10] However, the hypothesis for the reactive nature of CNKL may be challenged by the fact that some CNKL patients were proved to have a clonal proliferation in NK cells and/or to undergo transformation into NK cell leukemia/lymphoma.[11,12]

Making issues further complicated, the diagnostic criteria for CNKL are not clearly settled yet. Previous reports have proposed the requirement of sustained (>6 months) outgrowth of NK cells in PB ($>2.0\times10^9$ or $>0.6\times10^9$/l)[2,8] for the diagnosis of CNKL. However, NK cell count in the PB of CNKL individuals may fluctuate, and does not always fulfill the criteria. Morice *et al*[13] have reported that affected NK cells may have a restricted expression of a single isoform of killing inhibitory receptors (KIRs), supporting the usefulness of KIR expression as a clonality marker of NK cells.[13] However, these findings yet provide little information for the nature of affected NK cells in the CNKL condition.

DNA microarray enables us to measure the expression level for thousands of genes simultaneously,[14,15] and would be a promising tool to shed light from a new direction on the pathophysiology as well as diagnostic system for LDGL. Gene expression profiling with microarray has, for instance, succeeded in the differential diagnosis between acute myeloid leukemia (AML) and acute lymphoid leukemia (ALL), in extracting novel prognostic markers for prostate cancer,[16] and in the identification of molecular markers for myelodysplastic syndrome (MDS)[17] or chronic myeloid leukemia (CML).[18]

However, simple comparison of tissues or specimens may only yield pseudopositive and pseudonegative data. Although NK cells occupy 10–15% of PB mononuclear cells (MNCs) in healthy individuals, 80–90% of MNCs may be composed of affected NK cells in CNKL patients. If PB MNCs are simply compared between these two groups, any genes specific to NK cells would be considered to be activated in the latter. This misleading result may not reflect any changes in the amount of mRNA per NK cell. To minimize such pseudopositive/pseudonegative data, background-matched NK cell fractions should be purified from healthy individuals as well as LDGL patients prior to microarray analysis. Such approach, referred to as 'back-

Correspondence: Dr H Mano, Division of Functional Genomics, Jichi Medical School, 3311-1 Yakushiji, Kawachigun, Tochigi 329-0498, Japan; Fax: +81-285-44-7322; E-mail: hmano@jichi.ac.jp
This work was supported in part by a grant-in-aid for research on the second-term comprehensive 10-year strategy for cancer control from the Ministry of Health, Labor, and Welfare of Japan, by a grant from Mitsubishi Pharma Research Foundation, by a grant from Takeda Science Foundation, and by a grant from Sankyo Foundation of Life Science.
Received 12 August 2003; accepted 14 November 2003; Published online 22 January 2004

ground-matched population (BAMP) screening',[17] should pinpoint the gene expression alterations truly specific to each condition.

The efficacy of BAMP screening has been already demonstrated by Makishima *et al*[19] in the analysis of $CD4^-CD8^+$ T-cell type LDGL. $CD4^-CD8^+$ fractions were purified from PB MNCs of such LDGL patients and age-matched healthy volunteers, and were subjected to microarray analysis, resulting in the identification of novel molecular markers for T cell-type LDGL.

Analogously, here we isolated $CD3^-CD56^+$ NK cell fractions from healthy volunteers ($n=9$) as well as individuals with CNKL ($n=9$) or with ANKL ($n=1$). By using high-density oligonucleotide microarray, expression profiles for >12 000 human genes were obtained for these purified NK cell specimens. Analysis of the data set with sophisticated statistical methods has clarified that the affected NK cells are clearly distinct from normal ones, at least, with regard to transcriptome.

Materials and methods

Purification of $CD3^-CD56^+$ cells

PB MNCs were isolated by Ficoll–Hypaque density gradient centrifugation from the subjects with informed consent. The cells were incubated with anti-CD3 MicroBeads (Miltenyi Biotec, Auburn, CA, USA), and loaded onto MIDI-MACS magnetic cell separation columns (Miltenyi Biotec) to remove $CD3^+$ cells. The flow-through was then mixed with anti-CD56 MicroBeads (Miltenyi Biotec), and was subjected to a MINI-MACS column for the 'positive selection' of $CD56^+$ cells. Cells bound specifically to the column were then eluted according to the manufacturer's instructions, and stored in aliquots at −80°C.

Enrichment of $CD3^-CD56^+$ NK cell fraction was confirmed in every specimen by subjecting portions of the MNC and column eluates to staining with Wright–Giemsa solution and to the analysis of the cell surface expression of CD3 and CD56 by flow cytometry (FACScan; Becton Dickinson, Mountain View, CA, USA). The $CD3^-CD56^+$ fraction was shown to constitute >90% of each eluate of the affinity column.

DNA microarray analysis

Total RNA was extracted from the $CD3^-CD56^+$ cell preparations by the acid guanidinium method, and was subjected to two rounds of amplification with T7 RNA polymerase as described.[20] High fidelity of our RNA amplification procedure has been already reported.[18] The amplified cRNA (2 μg) was then converted to double-stranded cDNA, which was used to prepare biotin-labeled cRNA for hybridization with GeneChip HGU95Av2 microarrays (Affymetrix, Santa Clara, CA, USA) harboring oligonucleotides corresponding to a total of 12 625 genes. Hybridization, washing, and detection of signals on the arrays were performed with the GeneChip system (Affymetrix).

Class prediction by the 'weighted distance method'

The fluorescence intensity for each gene was normalized relative to the median fluorescence value of all human genes on the array in each hybridization. Hierarchical clustering of the data set and isolation of genes specific to the NK cells from healthy individuals (Normal) or to those of patients with LDGL were performed with GeneSpring 5.1 software (Silicon Genetics, Redwood, CA, USA).

In the comparison of normal- and LDGL-$CD3^-CD56^+$ cells, *t* statistic and effect size (difference in the mean of expression level between normal and LDGL classes)[16] were calculated for each gene. When a gene showed $|t|>3.966$ (corresponding to a significance level of 0.001 in *t*-test with 17 degrees of freedom) and |effect size| > 3, the difference in expression level between two classes was considered statistically significant. The genes showing the significant differences were called as 'informative genes' in this study. Correspondence analysis[21] was then performed with ViSta software (http://www.visualstats.org) for all genes showing a significant difference. Each sample was plotted in three dimensions, based on the coordinates obtained from the correspondence analysis.

To examine whether the informative genes were able to predict the class of the present specimens, we performed class prediction with our 'weighted distance method' (RO *et al*, submitted). This prediction method utilizes the dimensions obtained from correspondence analysis for the informative genes.

Consider a sample X to be predicted from N samples (excluding sample X) in the data set (N_A from class A and N_B from class B). Each sample can be represented by three dimensions, d_1, d_2, and d_3, where d_i denotes the coordinate in the ith dimension for the sample. The weighted distance from sample X to sample Y is defined as $D=\sqrt{\sum_{i=1}^{3}[v_i(d_i^X-d_i^Y)^2]}$, where v_i indicates the contribution of the ith dimension from correspondence analysis, and d_i^X and d_i^Y represent d_i for sample X and sample Y, respectively. Let D_A be the mean value of D from sample X to N_A samples belonging to class A, and D_B be the mean value of D from sample X to N_B samples belonging to class B. When $D_A/(D_A+D_B)<T$, the sample X is assigned class A, and when $D_B/(D_A+D_B)<T$, the sample X is assigned class B, where T is a threshold value. In our analysis, the T value was set to be 0.4. It should be noted that the weighted distance method could be applied to more than two classes.

In a cross-validation trial for the prediction of normal or CNKL class, the entire prediction process mentioned above was repeated for the 18 samples (nine for normal and nine for CNKL). To predict the class of every sample X, the correspondence analysis was carried out for the informative genes obtained from the remaining 17 samples. In this case, the informative genes were selected with a criteria of $|t|>4.073$ (corresponding to a significance level of 0.001 in *t*-test with 15 degrees of freedom) and |effect size| > 3.

All raw array data as well as details of the genes shown in the figures are available as supplementary information at the *Leukemia* web site.

'Real-time' reverse transcription-polymerase chain reaction (RT-PCR) analysis

Portions of nonamplified cDNA were subjected to PCR with a QuantiTect SYBR Green PCR Kit (Qiagen, Valencia, CA, USA). The amplification protocol comprised incubations at 94°C for 15 s, 60°C for 30 s, and 72°C for 60 s. Incorporation of the SYBR Green dye into PCR products was monitored in real time with an ABI PRISM 7700 sequence detection system (PE Applied Biosystems, Foster City, CA, USA), thereby allowing determination of the threshold cycle (C_T) at which exponential amplification of PCR products begins. The C_T values for cDNAs corresponding to the glyceraldehyde-3-phosphate dehydrogen-

ase (GAPDH) and interferon-γ (IFNG; GenBank accession number, X13274) genes were used to calculate the abundance of *IFNG* mRNA relative to that of *GAPDH* mRNA. The oligonucleotide primers for PCR were 5′-GTCAGTGGTG-GACCTGACCT-3′ and 5′-TGAGCTTGACAAAGTGGTCG-3′ for *GAPDH*, and 5′-GGGCCAACTAGGCAGCCAACTAA-3′ and 5′-GGAAGCACCAGGCATGAAATCTCC-3′ for *IFNG* cDNA.

Determination of serum level of IFNG protein

Sera were obtained from healthy volunteers and individuals with aplastic anemia (AA), systemic lupus erythematosus (SLE), virus infection-associated hemophagocytic syndrome (VAH), LDGL of $\alpha\beta^+$ T cell, LDGL of $\gamma\delta^+$ T cell, infectious mononucleosis (IMN), CNKL, or ANKL. The serum concentration of IFNG was determined by a flow cytometer with Human Th1/Th2 Cytokine Cytometric Bead Array Kit (BD Biosciences, San Diego, CA, USA) according to the manufacturer's protocols.

Results

Purification of NK cells

To directly compare the transcriptome of normal and affected NK cells, we here purified $CD3^-CD56^+$ fractions from PB MNCs of healthy volunteers ($n=9$) as well as of individuals with CNKL ($n=9$) or ANKL ($n=1$). A total of 19 specimens were thus registered into this study. The clinical characteristics of the 10 patients (CNKL-1～9 and ANKL-1) are summarized in Table 1. The LGL count in their PB was 14056 cells/ml±11695 (mean±s.d.). The proportion of $CD56^+$ cells in PB MNC was >50% in all affected individuals, indicating a predominant outgrowth of NK cells. All $CD56^+$ fractions in this study were negative for the surface expression of CD3.

The mono- or oligoclonal expansion with regard to EBV infection was confirmed in the NK cells of one CNKL (CNKL-9) and the ANKL (ANKL-1) patients. Importantly, the CNKL-9 patient with monoclonal expansion of EBV^+ NK cells died from leukemic transformation with infiltration into multiple organs at 24 months after the blood sampling. It is, therefore, likely that this patient might have been under a transition process toward ANKL or been at a very early stage of ANKL.

Magnetic bead-based affinity column has succeeded in a substantial enrichment of the NK cell fraction. In one healthy volunteer, for instance, PB MNCs was occupied with 12.3% of $CD3^-CD56^+$ fraction, while the column eluent contained 96.0% of those cells (Figure 1, upper panel). Similar purity of $CD3^-CD56^+$ fraction was also obtained for the patients with CNKL, as demonstrated in the lower panel. The purified cells exhibited a homogenous phenotype of LGL (Figure 1). Successful enrichment of NK cells (>90% purity) was confirmed in every case by flow cytometry and Wright–Giemsa staining of cytospin preparations (not shown). Cell number of the $CD3^-CD56^+$ fractions obtained in each individual was $3.9\times10^5\pm3.4\times10^5$ (mean±s.d.).

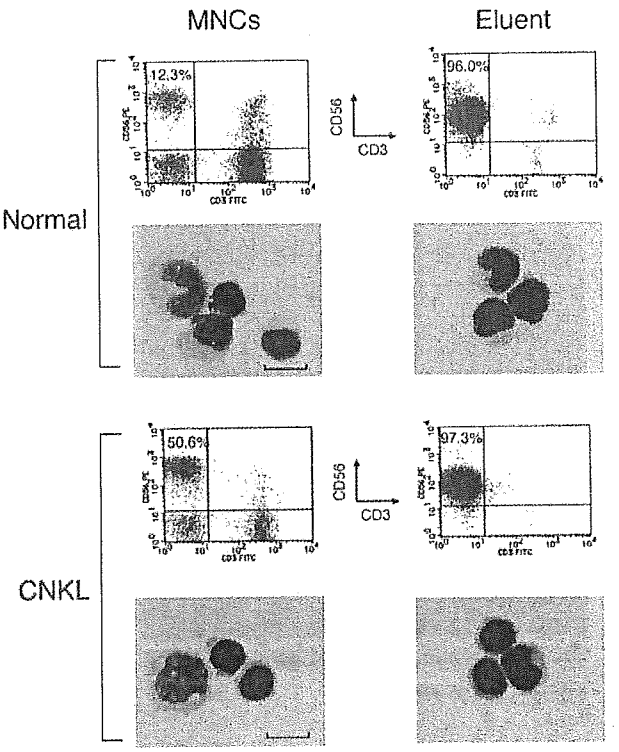

Figure 1 Purification of $CD3^-CD56^+$ fraction. MNCs isolated from PB of a healthy volunteer (normal) and a patient with CNKL were used to purify $CD3^-CD56^+$ fractions (Eluent). Cell surface expression of CD3 and CD56 was monitored in each fraction by flow cytometry, and the proportion (%) of $CD3^-CD56^+$ cells is indicated. Cytospin preparation of each fraction was stained with the Wright–Giemsa solutions. Scale bar, 50 μm.

Table 1 Clinical characteristics of the patients with NK cell-type LDGL

Patient	*Disease*	*Age*	*Sex*	*WBC (/mm³)*	*Lymph (/mm³)*	*LGL (/mm³)*	*Hb (g/dl)*	*Plt (×10⁴/mm³)*	*CD3⁺ (%)*	*CD5⁺ (%)*	*CD56⁺ (%)*	*EBV*
CNKL-1	CNKL	70	F	5880	4586	3927	14.6	24.1	13	13	78	–
CNKL-2	CNKL	54	M	10190	7133	6842	14.9	61.8	6	10	94	–
CNKL-3	CNKL	73	F	13780	11024	9721	13.2	24.9	9	7	91	n.d.
CNKL-4	CNKL	51	F	16500	11390	8420	13.1	25	21	23	76	n.d.
CNKL-5	CNKL	55	F	21100	17700	16880	13	17	10	9	79	n.d.
CNKL-6	CNKL	62	M	18000	11880	10252	13.1	39.6	13	13	86	n.d.
CNKL-7	CNKL	34	M	22100	13040	6590	16.4	31.2	35	n.d.	51	–
CNKL-8	CNKL	62	F	45400	43580	22250	11.7	16	3	3	82	n.d.
CNKL-9	CNKL	76	M	14800	13620	10510	11.2	5.8	12	9	75	+
ANKL-1	ANKL	15	F	51700	45760	41360	13.7	20.6	20	20	58	+

F, female; M, male; WBC, white blood cells; Lymph, lymphocytes; LGL, large granular lymphocytes; Hb, hemoglobin; Plt, platelets; n.d., not determined. Monoclonal or biclonal EBV genome was detected in the NK cells of CNKL-9 or ANKL-1 patient, respectively.

BAMP screening of NK cell fractions

Biotin-labeled cRNA was prepared from surface marker-matched NK fractions from the study subjects, and was hybridized with high-density oligonucleotide microarrays (Affymetrix HGU95Av2), providing the expression data for >12 000 human genes. To exclude genes that were virtually silent transcriptionally, we first selected genes whose expression received the 'Present' call from the Microarray Suite 4.0 software (Affymetrix) in at least 10% of the samples. A total of 6494 genes passed this 'selection window,' and their expression profiles in the 19 samples are shown in Figure 2a as a dendrogram, or 'gene tree,' in which genes with similar expression profiles (assessed by standard correlation) among the samples were clustered near each other. In Figure 2a, several clusters of genes that were expressed preferentially in either normal or affected NK cells (shown by arrows) were identified.

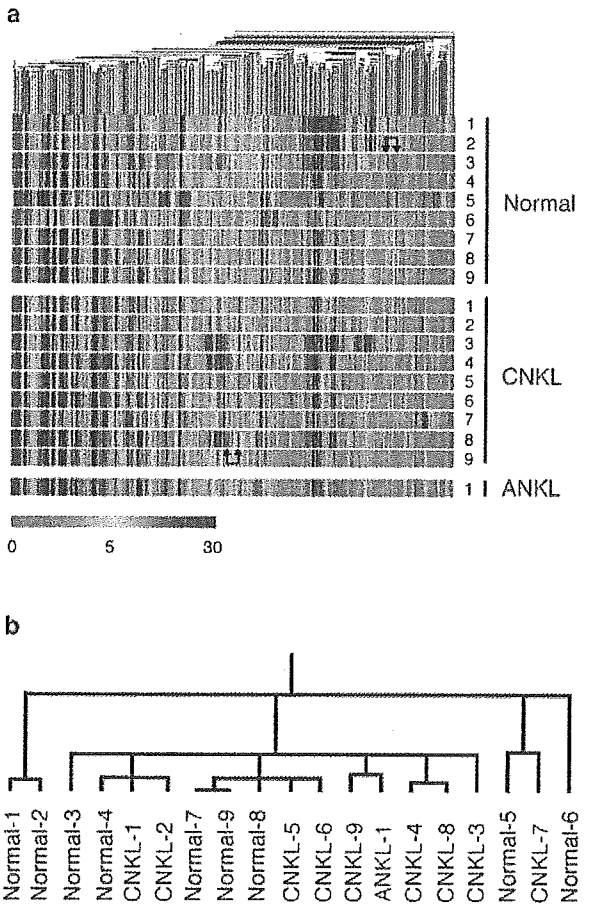

Figure 2 Expression profiles of 6494 genes in NK cell fractions. (a) Hierarchical clustering of 6494 genes on the basis of their expression profiles in $CD3^{-}CD56^{+}$ fractions derived from nine healthy volunteers (Normal), nine individuals with CNKL, and one with ANKL. Each column represents a single gene on the microarray, and each row a separate patient sample. Expression level of each gene is shown color-coded, as indicated by the scale at the bottom. Arrows indicate the positions of clusters of genes that were expressed preferentially in either normal or affected NK cells. (b) Two-way clustering analysis of the healthy individuals (Normal-1–9), CNKL patients (CNKL-1–9), and the ANKL patient (ANKL-1), based on the similarities in the expression profiles of the 6494 genes demonstrated in (a).

To statistically evaluate the similarity of the overall gene expression profiles across the 19 samples, we generated another dendrogram, a 'patient tree,' by the two-way clustering method,[22] with a separation ratio of 0.5 (Figure 2b). The samples did not clearly cluster into disease-specific branches; rather, normal and affected NK samples were mixed in several branches.

Identification of LDGL-associated genes

One of the major goals in this study was to develop expression profile-based diagnostic procedures for the NK cell disorders. For such an approach to be meaningful, an important question to be addressed would be thus to clarify whether affected NK cells share a specific gene expression profile, or 'molecular signature',[23] clearly distinct from that of normal NK cells.

Therefore, we first tried to identify genes whose expression level may efficiently differentiate normal NK cells from LDGL ones. For this purpose, we chose genes whose expression level differed significantly between the two groups of samples (Student's *t*-test, $P<0.001$). However, most of the genes thus identified had a low level of expression throughout all samples, making their usefulness as molecular markers uncertain. From these genes, therefore, we selected those whose mean expression intensity differed by $\geqslant 3.0$ arbitrary units (U) between the two groups. The resultant 15 'LDGL-associated genes' are shown in a gene tree format (Figure 3a); five of them were specific to CNKL/ANKL cells, while the remaining 10 genes were to normal NK cells.

The former group of the genes included those for transcriptional factors involved in the regulation of cell growth and/or apoptosis. B lymphoma Mo-MLV insertion region (BMI1; GenBank accession number, L13689), for example, belongs to the Polycomb type of DNA-binding proteins.[24] Intriguingly, BMI1 is expressed in hematopoietic stem cells (HSCs), and plays an indispensable role in the self-renewal process of HSCs.[25,26] Therefore, abundant expression of *BMI1* gene only in the affected NK cells may be involved in the deregulated outgrowth of the NK cells. Similarly, a zinc-finger protein ZFR (GenBank accession number, AI743507) was shown to protect embryonic cells from apoptosis and provide mitotic activity.[27]

Class prediction by our 'weighted distance method'

We next performed two-way clustering analysis, with a separation ratio of 0.5,. of the 19 specimens based on the expression levels of such 15 LDGL-associated genes. As shown in Figure 3b, the samples clustered into three major branches; one contains mainly normal NK specimens (with an addition of CNKL-1), another is composed solely of two CNKL patients (CNKL-2 and -7), and the other contains only affected NK cells. It should be noted that the ANKL sample was clustered closely with CNKL ones in the third branch.

Do the gene-expression profiles of NK cells differ between healthy individuals and those with NK cell disorders, and, if so, how different? Is such difference large enough to develop an expression profile-based diagnosis system? To address these issues, we performed correspondence analysis[21] to extract three major dimensions from the expression patterns of the 15 LDGL-associated genes. On the basis of the calculated three-dimensional coordinates for each sample, the specimens were then projected into a virtual space (Figure 3c). All normal samples were placed at a position clearly far from that of the

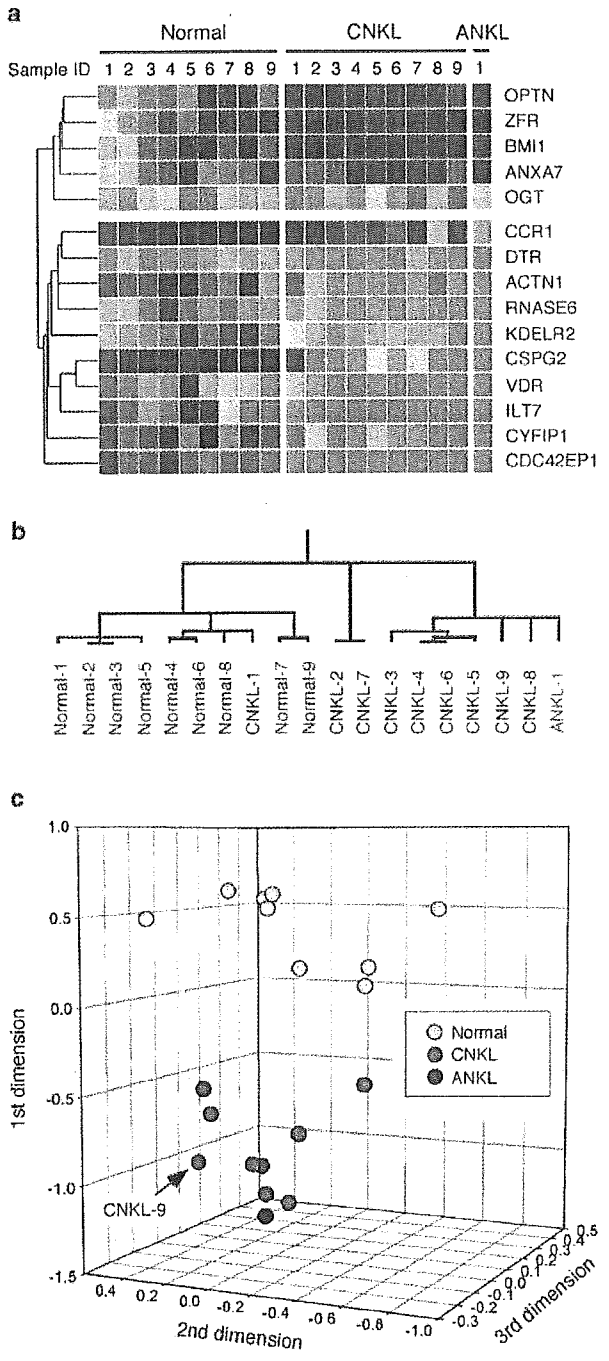

Figure 3 Identification of LDGL-associated genes. (a) Expression profiles of 15 LDGL-associated genes are shown in a dendrogram, color-coded as indicated by the scale in Figure 2a. Each row corresponds to a single gene, and each column to NK cells from healthy individuals (normal) and patients with CNKL or ANKL. The gene symbols are indicated on the right. The names, accession numbers, and expression intensity data for these genes are available at the *Leukemia* web site. (b) Two-way clustering analysis of the 19 samples based on the expression levels of the LDGL-associated genes. (c) Correspondence analysis of the LDGL-associated genes identified three major dimensions in their expression profiles. Projection of the specimens into a virtual space with these three dimensions revealed that the specimens from healthy individuals (normal) were clearly separated from those from the patients with CNKL or ANKL. The position of EBV$^+$ CNKL-9 sample is indicated.

affected NK cells, indicating that all affected NK cells possessed a common molecular signature which was distinct from that of the normal NK cells. Again, here the two samples with clonal EBV infection (CNKL-9 and ANKL-1) were placed closely with the other CNKL specimens.

The clear separation of affected NK specimens from normal ones in Figure 3c also supported the feasibility of an expression profile-based prediction for NK cell disorders. We therefore tried class prediction (normal or LDGL) for each specimen on the basis of the coordinates calculated by the correspondence analysis. The relative 'weighted distances' of a given specimen to the normal or LDGL group (excluding the specimen for the prediction) were calculated, and the specimen was assigned a class when the relative distance to the class was <0.4. As demonstrated in Table 2, our weighted-distance method could correctly predict the class of every sample examined, making the array-based diagnostic procedure of NK cell-type LDGL into reality.

Comparison of 'Normal vs *CNKL' by the weighted-distance method*

Given the large difference in the clinical course between CNKL and ANKL, there may be gene-expression alterations specific to the latter condition, which characterize its aggressive clinical course. Therefore, it might be appropriate to investigate these two conditions separately. We thus focused on the comparison between normal individuals and those with CNKL, and tried to assign, by the weighted-distance method, either normal or CNKL class to every specimen among nine healthy individuals and nine patients with CNKL.

To accurately measure the prediction power of our weighted-distance method, we conducted a cross-validation trial (i.e., 'drop-one-out' format) for the diagnosis of normal or CNKL class. To predict the class of sample X, 'CNKL-associated genes' were extracted from the comparison of remaining 17 samples

Table 2 Diagnosis by the 'weighted-distance method'

Patient ID	*Clinical diagnosis*	*Distance to normal*	*Distance to LDGL*	*Prediction*
Normal-1	Normal	0.207	0.793	Normal
Normal-2	Normal	0.256	0.744	Normal
Normal-3	Normal	0.192	0.808	Normal
Normal-4	Normal	0.200	0.800	Normal
Normal-5	Normal	0.211	0.789	Normal
Normal-6	Normal	0.229	0.771	Normal
Normal-7	Normal	0.311	0.689	Normal
Normal-8	Normal	0.352	0.648	Normal
Normal-9	Normal	0.391	0.609	Normal
CNKL-1	LDGL	0.729	0.271	LDGL
CNKL-2	LDGL	0.845	0.155	LDGL
CNKL-3	LDGL	0.854	0.146	LDGL
CNKL-4	LDGL	0.877	0.123	LDGL
CNKL-5	LDGL	0.800	0.200	LDGL
CNKL-6	LDGL	0.877	0.123	LDGL
CNKL-7	LDGL	0.735	0.265	LDGL
CNKL-8	LDGL	0.861	0.139	LDGL
CNKL-9	LDGL	0.868	0.132	LDGL
ANKL-1	LDGL	0.842	0.158	LDGL

The relative weighted distance to the normal group (distance to normal) or to LDGL group (distance to LDGL) was calculated, and used to assign a class (normal or LDGL) to each sample.

according to the criteria used in Figure 3a ($P<0.001$ in Student's *t*-test, and |effect size|>3). The number of such CNKL-associated genes ranged from 4 to 10. Correspondence analysis was carried out for the expression profiles of the CNKL-associated genes, and was used to calculate the relative weighted distance of the 'dropped' sample X to either normal or CNKL class. As shown in Table 3, with a *T*-value of 0.4, a clinically matched prediction was obtained for 14 (77.8%) out of 18 cases, while one case (CNKL-2) was unpredictable and three cases (normal-6, normal-8 and CNKL-1) received a prediction incompatible with the clinical diagnosis. Therefore, even in a cross-validation assay, the weighted-distance method could achieve a high accuracy.

For comparison, we also conducted a cross-validation trial of class prediction by using a known prediction algorithm, the '*k*-nearest neighbor method' (http://www.silicongenetics.com/Support/GeneSpring/GSnotes/class_prediction.pdf). Among the 18 samples tested, only 10 samples (55.6%) received correct prediction, indicating the superiority of our weighted distance method.

Since CNKL-9 patient had NK cells with EBV in a clonal episomal form, and had progressed into an ANKL phase in a relatively short period, we questioned if this patient had an atypical molecular signature for CNKL. To visualize the similarity of transcriptome of CNKL-9 sample with that of the other CNKL ones, the result of the cross-validation trial for CNKL-9 is demonstrated as a virtual-space format in Figure 4a. Correspondence analysis of nine genes that most efficiently differentiated normal-1–9 from CNKL-1–8 has identified three major dimensions in their expression pattern, and projection of the CNKL-9 patient together with the other samples in a 3D space indicated that CNKL-9 had an expression profile highly similar to that of the other CNKL subjects at least in the space of these nine highly informative genes.

To confirm the similarity in the gene-expression profile of EBV$^+$ ANKL cells to the CNKL ones, we next carried out correspondence analysis for the ANKL-1 patient. Statistical comparison of transcriptome between Normal-1–9 and CNKL-1–9 subjects identified a total of seven genes, which contrasted the expression profile of normal NK cells from that of CNKL NK cells. As shown in Figure 4b, projection of the ANKL-1 patient into a 3D space constructed from the data of such seven genes demonstrated that the EBV$^+$ ANKL-1 sample was plotted at a neighbor position to those of the CNKL samples. In accordance with the 3D view, the weighted-distance method also concluded that the ANKL-1 sample belonged to the same class with the CNKL ones (data not shown). These analyses unexpectedly suggested that the gene expression profile characteristic to CNKL NK cells is also shared with EBV$^+$ NK cells. It should be noted, however, that additional genetic changes specific to EBV infection may exist, and account for the fulminant clinical character of EBV$^+$ LDGL.

Table 3 Cross-validation of disease prediction

Patient ID	*Clinical diagnosis*	*Prediction*
Normal-1	Normal	Normal
Normal-2	Normal	Normal
Normal-3	Normal	Normal
Normal-4	Normal	Normal
Normal-5	Normal	Normal
Normal-6	Normal	CNKL
Normal-7	Normal	Normal
Normal-8	Normal	CNKL
Normal-9	Normal	Normal
CNKL-1	CNKL	Normal
CNKL-2	CNKL	Unpredictable
CNKL-3	CNKL	CNKL
CNKL-4	CNKL	CNKL
CNKL-5	CNKL	CNKL
CNKL-6	CNKL	CNKL
CNKL-7	CNKL	CNKL
CNKL-8	CNKL	CNKL
CNKL-9	CNKL	CNKL

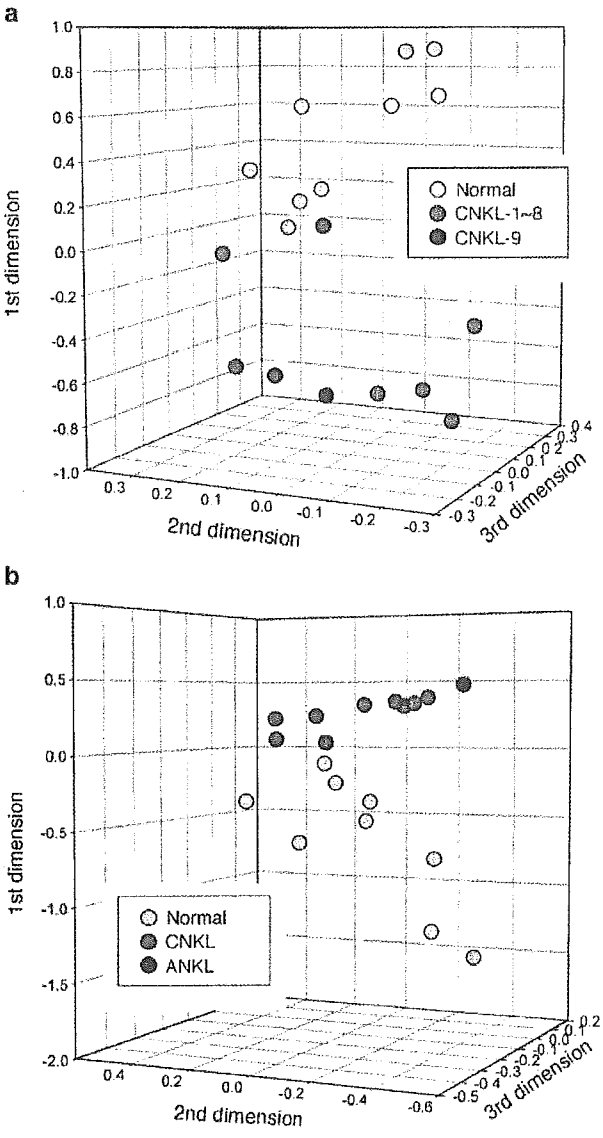

Figure 4 Investigation of the EBV$^+$ samples. (a) We could isolate nine genes, expression of which differentiated normal NK cells (normal) from indolent CNKL ones (CNKL-1–8). The EBV$^+$ CNKL-9 was projected into a virtual space together with the other normal and CNKL specimens, based on the coordinates calculated by the correspondence analysis of such nine genes. (b) A total of seven genes were identified to be differentially expressed between normal NK cells (normal) and CNKL cells. The ANKL-1 sample was projected into the virtual space as in (a).

Isolation of single-gene markers for LDGL diagnosis

The gene set identified in Figure 3a may potentially be the candidate genes to construct custom-made DNA microarrays for disease diagnosis of NK cell disorders. Since availability of DNA microarray systems is still restricted in current hospitals, however, it would be valuable if a high expression of single gene or its product can be used as a reliable marker for such purposes. For instance, it would be highly useful if the serum level of a protein can help to diagnose NK cell disorders. Given the presence of false data even with DNA microarray, it is unlikely that an expression of any single gene can correctly diagnose all samples. Therefore, here we have tried to isolate genes whose high expression may be 'sufficient' to predict the presence of NK cell-type LDGL, but the absence of its expression may not necessarily mean that the NK cells are normal. Such type of predictor genes should be strictly inactivated in all normal NK cells, but become activated in, at least, a part of the NK cells in the LDGL group.

To screen such type of predictors, first, the mean expression value of each gene was calculated for the normal or LDGL group. Then, with the use of GeneSpring software, we searched for genes whose expression profiles were statistically similar, with a minimum correlation of 0.95, to that of a hypothetical 'LDGL-specific gene' that exhibits a mean expression level of 0.0 U in the normal group and 100.0 U in the LDGL group. From such 652 genes identified, we then applied another criteria that gene-expression value should be (i) $\geqslant$60.0 U in, at least, one of the LDGL samples, and (ii) $<$25.0 U in all normal samples. A total of six genes were finally identified to be 'LDGL-specific' (Figure 5a). Here we have tried to extract LDGL-specific genes with minimum false-positive results, while allowing false-negative ones. Therefore, we should confidently tell that the given NK cells are of LDGL if one of the 'LDGL-specific genes' is highly expressed in the specimens.

Conversely, we also tried to identify 'normal-specific genes' through the same approach. Firstly, a total of 1424 genes were identified to be statistically similar to a hypothesized 'normal-specific gene' that has a mean expression value of 100.0 U in the normal group, but of 0.0 U in the LDGL group. Among these genes, those whose expression was kept below 25.0 U throughout the samples in the LDGL group, but became activated at $\geqslant$60.0 U in, at least, one sample in the normal group were selected. We could thus extract a set of 22 genes, expression of which was specific to normal NK cells (Figure 5b).

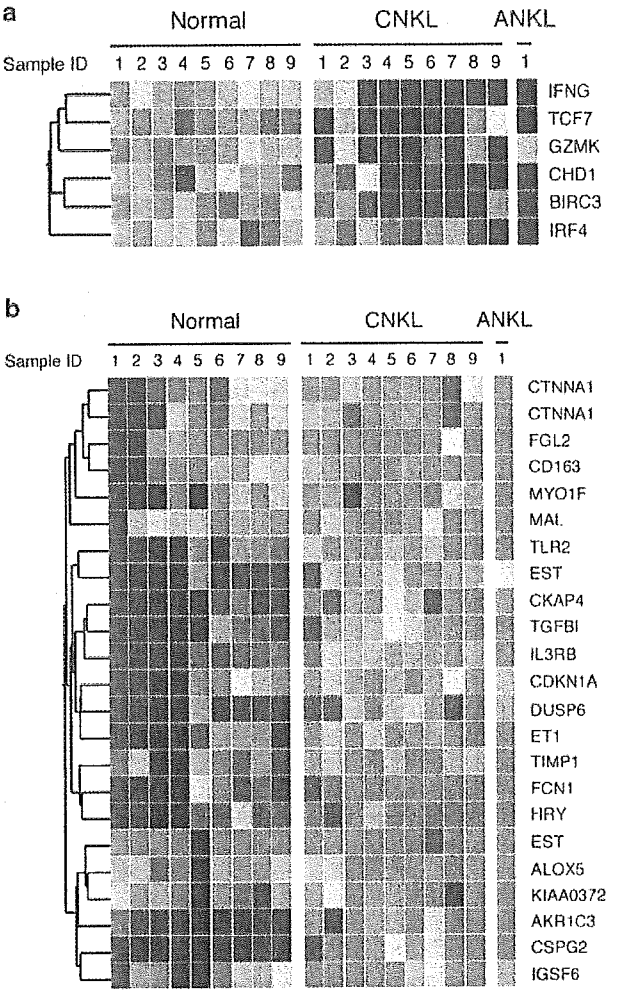

Figure 5 Identification of single-gene markers for LDGL. (a) Dendrogram showing the expression profiles of six genes whose expression intensity was kept suppressed in normal NK cells, but became activated in a part of affected NK cells. Each row represents a single gene, and each column a separate patient sample. Expression level of the genes is shown colored according to the scale in Figure 2a. (b) Expression profiles of 22 'normal-specific genes' are demonstrated as in (a). Two different oligonucleotide sets for the alphaE-catenin (CTNNA1) gene are present on an HGU95Av2 array.

Confirmation of overproduction of IFNG

NK cells become activated and produce IFNG in response to the stimulation with IL-2,[28] IL-12,[29] and IL-15.[30] Under physiological circumstances, however, activated NK cells eventually undergo apoptotic changes to prevent overactivation of the immune system. Interestingly, IFNG itself provides a survival signal onto NK cells, and, therefore, sustained incubation with IFNG of NK cells protects efficiently them from cell death.[31] It was thus provocative to find *IFNG* in our LDGL-specific genes (Figure 5a), indicating a potential role of IFNG in the outgrowth mechanism of NK cells in the LDGL condition.

Here we have confirmed the disease-specific expression of *IFNG* gene by a quantitative 'real-time' RT-PCR assay. As shown in Figure 6a, abundant expression of *IFNG* mRNA was only detected in the purified NK cell fraction of LDGL patients, but not of the normal controls. Furthermore, a high concentration of IFNG protein was also observed in the sera of CNKL/ANKL patients (Figure 6b), proving that overexpression of *IFNG* mRNA in NK cell disorders leads to the systemic elevation of IFNG protein level. Interestingly, overexpression of IFNG protein was also noticed in the patients with IMN. High expression of IFNG in IMN individuals may result from the infection of EBV associated with IMN, or may indicate the activated status of T or NK cells in the condition of IMN.

Discussion

In this manuscript, we tried to clarify whether gene-expression profiling can help to differentiate NK cells of LDGL individuals from those of healthy ones. Toward this goal, we first purified NK cell fractions from study subjects, which are characterized by the absence of cell surface CD3 molecule and the presence of CD56 antigen. Analysis with these isolated NK cells should be

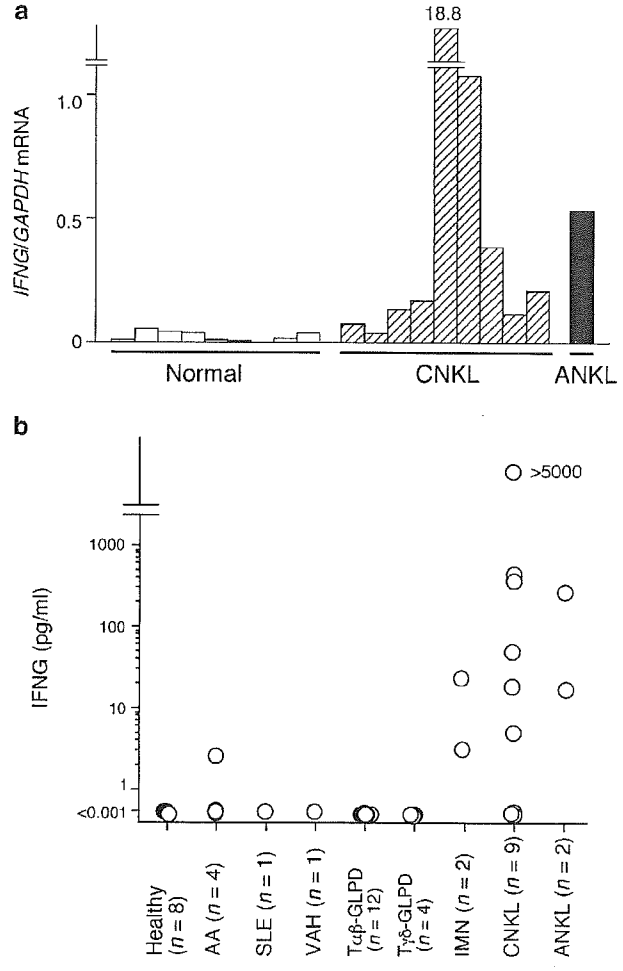

Figure 6 Confirmation of overexpression of IFNG. (a) Quantitation of *IFNG* mRNA in NK cell fractions. Complementary DNA was prepared from the NK cell fractions, and was subjected to real-time RT-PCR analysis with primers specific for the *IFNG* or *GAPDH* genes. The ratio of the abundance of *IFNG* mRNA to that of *GAPDH* mRNA was calculated as 2^n, where n is the C_T value for *GAPDH* cDNA minus the C_T value for *IFNG* cDNA. (b) Sera were obtained from healthy volunteers (healthy) and individuals with aplastic anemia (AA), systemic lupus erythematosus (SLE), virus infection-associated hemophagocytic syndrome (VAH), LDGL of $\alpha\beta^+$ T cell, LDGL of $\gamma\delta^+$ T cell, infectious mononucleosis (IMN), CNKL, or ANKL. The expression level of IFNG protein in the sera was determined by flow cytometry, and shown as pg/ml.

intrinsic for an accurate comparison of the disease status, since simple comparison with PB MNCs would be severely influenced by any changes in the cell composition of PB MNCs in each individual.

However, even by using expression profiles of the purified fractions, similarity of the expression pattern of all gene set failed to clearly separate the affected NK cells from normal ones (Figure 2b), indicating the necessity of a diagnostic system with a 'supervised' algorithm. For this aim, we first extracted gene clusters, expression of which was specific to either normal or affected NK cells. Correspondence analysis on the expression patterns of such 'LDGL-associated genes' has succeeded in the reduction of the number of pattern dimensions into three. To our surprise, projection of all samples into this 3D space clearly demonstrated that the affected NK cells (CNKL/ANKL) were placed clustered at a position separate from that of normal NK cells (Figure 3c). With coordinates in such decomposited dimensions, we then invented a novel class prediction means, 'weighted-distance method'. As expected from the clear separation in the 3D view, the weighted-distance method provided correct prediction for all samples studied. A cross-validation trial for the disease diagnosis also gave a highly accurate prediction rate (77.8%).

Given a high incidence of clonal EBV infection in ANKL cells, EBV is believed to play an essential role in the pathogenesis of this fulminant disorder. From the point of view of gene-expression profile, the NK cells positive for EBV infection (CNKL-9 and ANKL-1) shared gene-expression patterns characteristic to other indolent CNKL cells. For instance, a comparison of normal NK cells and CNKL samples (except EBV^+ CNKL-9) has identified a total of nine CNKL-related genes including those for nuclear matrix protein-2 (GenBank accession number, D50926), cytochrome *C* (D00265), tyrosine 3-monooxygenase/tryptophan 5-monooxygenase activation protein, theta polypeptide or 14-3-3 protein tau (X56468), O-linked GlcNAc transferase (AL050366), IFNG, chemokine C–C motif receptor 1 (CCR1; D10925), chondroitin sulfate proteoglycan 2 (X15998), and fibrinogen-like 2 (AI432401). The 3D view of the correspondence analysis for these 'CNKL-associated' genes clearly demonstrated that the EBV^+ CNKL-9 subject was included in the other indolent CNKL group (Figure 4a). Similarly, another EBV^+ subject (ANKL-1) was placed closely with the CNKL samples, according to the expression profiles of the genes which differentiated CNKL cells from normal NK cells (Figure 4b).

These data propose a hypothesis that gene-expression alterations characteristic to an activated, yet indolent, proliferation of NK cells found in CNKL patients also take place in the highly proliferating NK cells in EBV^+ individuals. In other words, a similar mechanism may be utilized for the sustained outgrowth of NK cells both in the individuals with CNKL and ANKL. It should be emphasized, however, that the number of EBV^+ samples ($n=2$) in these analyses was too small to extract any conclusive remarks on the pathophysiology of proliferating EBV^+ NK cells. Nevertheless, we believe that it was interesting to find that EBV^+ NK cells may share a molecular signature with EBV^- LDGL cells.

We finally tried to identify single-gene markers, the presence or absence of which helps the diagnosis of LDGL. A total of 22 genes were shown to be specific to normal NK cells, including those for cyclin-dependent kinase inhibitor 1A (CDKN1A; GenBank accession number U03106) or CIP1, dual-specificity phosphatase 6 (DUSP6; AB013382), toll-like receptor 2 (TLR2; AF051152), tissue inhibitor of metalloproteinase 1 (TIMP1; D11139), and aldo-keto reductase family 1 member C3 (AKR1C3; D17793) (Figure 5b).

CDKN1A is transcriptionally regulated by the activity of p53, and functions as a major effector for antitumor activity of p53, through the suppression of cyclin-dependent kinase activities.[32] Therefore, loss of expression of *CDKN1A* may allow uncontrolled transition at the G_2–M boundary in the cell cycle, and may partially account for the overgrowth of NK cells in LDGL individuals. Similarly, DUSP6 antagonizes MAPK activities *via* dephosphorylation of the latter kinases.[33] Decrease of DUSP6 expression may therefore contribute to overactivation of MAPK and to enhanced mitogenesis.

AKR1C3 catalyzes conversion of aldehydes and ketones to alcohols *in vivo*. Although its role in NK cells is unknown yet, downregulation of its transcription has been also reported in the

LGLs of T cell-type LDGL.[19] Comparison with DNA microarray of $CD4^{-}CD8^{+}$ T-cells between healthy individuals and those with T cell-type LDGL has identified the *AKR1C3* gene as the specific marker to the former. Decrease of *AKR1C3* message was also confirmed by quantitative 'real-time' RT-PCR method in those patients. Transcriptional suppression of *AKR1C3* was thus revealed in affected LGLs for both NK cell- and T cell-type LDGL, and may be a common marker for the diagnosis of LDGL condition.

A number of growth-promoting factors were found in the 'LDGL-specific genes' in Figure 5a. IFNG and BIRC3[34] are, for instance, known to protect NK cells from apoptosis, and IRF4 has an oncogenic activity *in vivo*.[35] Additionally, CHD1 contains an SNF2-related helicase/ATPase domain, and is presumed to be involved in the regulation of chromatin structure and gene transcription as well.[36]

Our data, together with that by Mizuno *et al*[31] suggest that the serum concentration of IFNG protein may be an indicator of NK cell-type LDGL. Direct production of IFNG by affected NK cells may also imply the presence of an autocrine loop for the NK cell growth.

The mechanism by which affected NK cells produce IFNG is still to be revealed. It is known that IL-2, IL-12, IL-15, and IL-18 all activate production of IFNG in NK cells. In our microarray data set, however, none of IL-2, IL-12, and IL-18 were found to be significantly expressed in the subjects (not shown). Although IL-15 was moderately expressed in our NK samples, its expression level did not differ between normal and affected NK cells. In support of this notion, we could not detect significant level of IL-2 protein in the examination of serum level of cytokines (not shown). Therefore, it is currently an open question as to whether activation of *IFNG* transcription in the affected NK cells is a secondary event from the stimulation by other cells such as T cells, or intracellular mechanism of IFNG expression is deregulated in the affected NK cells.

Conclusion

We have characterized the transcriptome of a relatively uncommon disorder, NK cell-type LDGL. Comparison of purified NK cells between healthy and CNKL individuals led to the identification of gene sets which are useful in the expression profile-based differential diagnosis of the disorder. Such disease-associated genes have also provided us insights into the molecular pathogenesis of NK cell-type LDGL. Together with further optimization of statistical methods, increase in the number of both genes and subjects for the analysis would help to define and clarify the clinical entities of NK cell disorders.

Acknowledgements

We thank all patients, healthy volunteers, and physicians who participated in the collection of NK cell depository. We are also grateful to Dr T Miwa for his helpful suggestions.

Supplementary Information

Supplementary Information accompanies the paper on the Leukemia website (http://www.nature.com/leu).

References

1 Loughran Jr TP. Clonal diseases of large granular lymphocytes. *Blood* 1993; **82**: 1–14.
2 Semenzato G, Zambello R, Starkebaum G, Oshimi K, Loughran Jr TP. The lymphoproliferative disease of granular lymphocytes: updated criteria for diagnosis. *Blood* 1997; **89**: 256–260.
3 Oshimi K. Granular lymphocyte proliferative disorders: report of 12 cases and review of the literature. *Leukemia* 1988; **2**: 617–627.
4 Loughran Jr TP, Starkebaum G. Large granular lymphocyte leukemia. Report of 38 cases and review of the literature. *Medicine (Baltimore)* 1987; **66**: 397–405.
5 Jaffe ES, Harris NL, Stein H, Vardiman JW (eds). *Pathology and Genetics of Tumours of Haematopoietic and Lymphoid Tissues*. Lyon: IARC Press, 2001.
6 Gelb AB, van de Rijn M, Regula Jr DP, Cornbleet JP, Kamel OW, Horoupian DS *et al*. Epstein–Barr virus-associated natural killer-large granular lymphocyte leukemia. *Hum Pathol* 1994; **25**: 953–960.
7 Tefferi A. Chronic natural killer cell lymphocytosis. *Leuk Lymphoma* 1996; **20**: 245–248.
8 Rabbani GR, Phyliky RL, Tefferi A. A long-term study of patients with chronic natural killer cell lymphocytosis. *Br J Haematol* 1999; **106**: 960–966.
9 Nash R, McSweeney P, Zambello R, Semenzato G, Loughran Jr TP. Clonal studies of CD3-lymphoproliferative disease of granular lymphocytes. *Blood* 1993; **81**: 2363–2368.
10 Garcia-Suarez J, Prieto A, Reyes E, Arribalzaga K, Perez-Machado MA, Lopez-Rubio M *et al*. Persistent lymphocytosis of natural killer cells in autoimmune thrombocytopenic purpura (ATP) patients after splenectomy. *Br J Haematol* 1995; **89**: 653–655.
11 Ohno Y, Amakawa R, Fukuhara S, Huang CR, Kamesaki H, Amano H *et al*. Acute transformation of chronic large granular lymphocyte leukemia associated with additional chromosome abnormality. *Cancer* 1989; **64**: 63–67.
12 Tefferi A, Greipp PR, Leibson PJ, Thibodeau SN. Demonstration of clonality, by X-linked DNA analysis, in chronic natural killer cell lymphocytosis and successful therapy with oral cyclophosphamide. *Leukemia* 1992; **6**: 477–480.
13 Morice WG, Kurtin PJ, Leibson PJ, Tefferi A, Hanson CA. Demonstration of aberrant T-cell and natural killer-cell antigen expression in all cases of granular lymphocytic leukaemia. *Br J Haematol* 2003; **120**: 1026–1036.
14 Cheung VG, Morley M, Aguilar F, Massimi A, Kucherlapati R, Childs G. Making and reading microarrays. *Nat Genet* 1999; **21**: 15–19.
15 Duggan DJ, Bittner M, Chen Y, Meltzer P, Trent JM. Expression profiling using cDNA microarrays. *Nat Genet* 1999; **21**: 10–14.
16 Dhanasekaran SM, Barrette TR, Ghosh D, Shah R, Varambally S, Kurachi K *et al*. Delineation of prognostic biomarkers in prostate cancer. *Nature* 2001; **412**: 822–826.
17 Miyazato A, Ueno S, Ohmine K, Ueda M, Yoshida K, Yamashita Y *et al*. Identification of myelodysplastic syndrome-specific genes by DNA microarray analysis with purified hematopoietic stem cell fraction. *Blood* 2001; **98**: 422–427.
18 Ohmine K, Ota J, Ueda M, Ueno S-i, Yoshida K, Yamashita Y *et al*. Characterization of stage progression in chronic myeloid leukemia by DNA microarray with purified hematopoietic stem cells. *Oncogene* 2001; **20**: 8249–8257.
19 Makishima H, Ishida F, Ito T, Kitano K, Ueno S, Ohmine K *et al*. DNA microarray analysis of T cell-type lymphoproliferative disease of granular lymphocytes. *Br J Haematol* 2002; **118**: 462–469.
20 Van Gelder RN, von Zastrow ME, Yool A, Dement WC, Barchas JD, Eberwine JH. Amplified RNA synthesized from limited quantities of heterogeneous cDNA. *Proc Natl Acad Sci USA* 1990; **87**: 1663–1667.
21 Fellenberg K, Hauser NC, Brors B, Neutzner A, Hoheisel JD, Vingron M. Correspondence analysis applied to microarray data. *Proc Natl Acad Sci USA* 2001; **98**: 10781–10786.
22 Alon U, Barkai N, Notterman DA, Gish K, Ybarra S, Mack D *et al*. Broad patterns of gene expression revealed by clustering analysis of tumor and normal colon tissues probed by oligonucleotide arrays. *Proc Natl Acad Sci USA* 1999; **96**: 6745–6750.

23 Ramaswamy S, Ross KN, Lander ES, Golub TR. A molecular signature of metastasis in primary solid tumors. *Nat Genet* 2003; **33**: 49–54.
24 Alkema MJ, Wiegant J, Raap AK, Berns A, van Lohuizen M. Characterization and chromosomal localization of the human proto-oncogene BMI-1. *Hum Mol Genet* 1993; **2**: 1597–1603.
25 Park IK, Qian D, Kiel M, Becker MW, Pihalja M, Weissman IL *et al*. Bmi-1 is required for maintenance of adult self-renewing haematopoietic stem cells. *Nature* 2003; **423**: 302–305.
26 Lessard J, Sauvageau G. Bmi-1 determines the proliferative capacity of normal and leukaemic stem cells. *Nature* 2003; **423**: 255–260.
27 Meagher MJ, Braun RE. Requirement for the murine zinc finger protein ZFR in perigastrulation growth and survival. *Mol Cell Biol* 2001; **21**: 2880–2890.
28 Thornton S, Kuhn KA, Finkelman FD, Hirsch R. NK cells secrete high levels of IFN-gamma in response to in vivo administration of IL-2. *Eur J Immunol* 2001; **31**: 3355–3360.
29 Ross ME, Caligiuri MA. Cytokine-induced apoptosis of human natural killer cells identifies a novel mechanism to regulate the innate immune response. *Blood* 1997; **89**: 910–918.
30 Carson WE, Giri JG, Lindemann MJ, Linett ML, Ahdieh M, Paxton R *et al*. Interleukin (IL) 15 is a novel cytokine that activates human natural killer cells via components of the IL-2 receptor. *J Exp Med* 1994; **180**: 1395–1403.
31 Mizuno S, Akashi K, Ohshima K, Iwasaki H, Miyamoto T, Uchida N *et al*. Interferon-gamma prevents apoptosis in Epstein–Barr virus-infected natural killer cell leukemia in an autocrine fashion. *Blood* 1999; **93**: 3494–3504.
32 El-Deiry WS, Tokino T, Velculescu VE, Levy DB, Parsons R, Trent JM *et al*. WAF1, a potential mediator of p53 tumor suppression. *Cell* 1993; **75**: 817–825.
33 Muda M, Boschert U, Dickinson R, Martinou JC, Martinou I, Camps M *et al*. MKP-3, a novel cytosolic protein-tyrosine phosphatase that exemplifies a new class of mitogen-activated protein kinase phosphatase. *J Biol Chem* 1996; **271**: 4319–4326.
34 Liston P, Roy N, Tamai K, Lefebvre C, Baird S, Cherton-Horvat G *et al*. Suppression of apoptosis in mammalian cells by NAIP and a related family of IAP genes. *Nature* 1996; **379**: 349–353.
35 Iida S, Rao PH, Butler M, Corradini P, Boccadoro M, Klein B *et al*. Deregulation of MUM1/IRF4 by chromosomal translocation in multiple myeloma. *Nat Genet* 1997; **17**: 226–230.
36 Woodage T, Basrai MA, Baxevanis AD, Hieter P, Collins FS. Characterization of the CHD family of proteins. *Proc Natl Acad Sci USA* 1997; **94**: 11472–11477.